The Astrophysical Journal Supplement Series, 167:343–356, 2006 December

COLLISIONAL IONIZATION EQUILIBRIUM FOR OPTICALLY THIN PLASMAS. I. UPDATED RECOMBINATION RATE COEFFICIENTS FOR BARE THROUGH SODIUM-LIKE IONS

P. Bryans,[1] N. R. Badnell,[2] T. W. Gorczyca,[3] J. M. Laming,[4] W. Mitthumsiri,[1] and D. W. Savin[1]

Received 2006 April 17; accepted 2006 June 26

ABSTRACT

Reliably interpreting spectra from electron-ionized cosmic plasmas requires accurate ionization balance calculations for the plasma in question. However, much of the atomic data needed for these calculations have not been generated using modern theoretical methods and are often highly suspect. This translates directly into the reliability of the collisional ionization equilibrium (CIE) calculations. We make use of state-of-the-art calculations of dielectronic recombination (DR) rate coefficients for the hydrogenic through Na-like ions of all elements from He up to and including Zn. Where measurements exist, these published theoretical DR data agree with recent laboratory work to within typically 35% or better at the temperatures relevant for CIE. We also make use of state-of-the-art radiative recombination (RR) rate coefficient calculations for the bare through Na-like ions of all elements from H through to Zn. Here we present improved CIE calculations for temperatures from 10^4 to 10^9 K using our data and the recommended electron impact ionization data of Mazzotta et al. for elements up to and including Ni and Mazzotta for Cu and Zn. DR and RR data for ionization stages that have not been updated are also taken from these two additional sources. We compare our calculated fractional ionic abundances using these data with those presented by Mazzotta et al. for all elements from H to Ni. The differences in peak fractional abundance are up to 60%. We also compare with the fractional ionic abundances for Mg, Si, S, Ar, Ca, Fe, and Ni derived from the modern DR calculations of Gu for the H-like through Na-like ions, and the RR calculations of Gu for the bare through F-like ions. These results are in better agreement with our work, with differences in peak fractional abundance of less than 10%.

Subject headings: atomic data — atomic processes — plasmas

Online material: extended figure sets, machine-readable tables

1. INTRODUCTION

Electron ionized plasmas (also called collisionally ionized plasmas) are formed in a diverse variety of objects in the universe. These range from stellar coronae and supernova remnants through to the interstellar medium and gas in galaxies or in clusters of galaxies. The physical properties of these sources can be determined using spectral observations coupled with theoretical models. This allows one to infer electron and ion temperatures, densities, emission measure distributions, and ion and elemental abundances. However, reliably determining these properties requires accurate fractional abundance calculations for the different ionization stages of the various elements in the plasma (i.e., the ionization balance of the gas).

Since many of the observed sources are not in local thermodynamic equilibrium, in order to determine the ionization balance of the plasma one needs to know the rate coefficients for all the relevant recombination and ionization processes. Often, the observed systems are optically thin, low-density, dust-free, and in steady state or quasi–steady state. Under these conditions the effects of any radiation field can be ignored, density effects are insignificant, three-body collisions are unimportant, and the ionization balance of the gas is time-independent. This is commonly called collisional ionization equilibrium (CIE) or sometimes coronal equilibrium.

[1] Columbia Astrophysics Laboratory, Columbia University, New York, NY 10027.
[2] Department of Physics, University of Strathclyde, Glasgow, G4 0NG, UK.
[3] Department of Physics, Western Michigan University, Kalamazoo, MI 49008.
[4] E. O. Hulburt Center for Space Research, US Naval Research Laboratory, Code 7674L, Washington, DC 20375.

Because CIE occurs in a wide range of cosmic sources, accurate calculations have long been an issue of concern. One of the continuing challenges of theoretical and experimental atomic physics is to provide reliable data for all the relevant collision processes. In CIE, recombination is due to dielectronic recombination (DR) and radiative recombination (RR). At the temperature of peak formation in CIE, DR dominates over RR for most ions. Ionization is a result of electron impact ionization (EII). At temperatures low enough for both atoms and ions to exist, charge transfer (CT) can be both an important recombination and ionization process. Considering all the ions and levels that need to be taken into account, it is clear that vast quantities of data are needed. Generating them to the accuracy required pushes theoretical and experimental methods to the edge of what is currently achievable and often beyond. For this reason progress has been slow.

Over the years a number of different groups have evaluated the available atomic data and produced CIE calculations. Some of the most commonly cited results are those of Shull & van Steenberg (1982), Arnaud & Rothenflug (1985), Landi & Monsignori Fossi (1991), Arnaud & Raymond (1992), and Mazzotta et al. (1998). Masai (1997) investigated the astrophysical implications for several different CIE models on the fractional abundance of Fe. More recently, Gu (2003b) carried out CIE calculations using his DR and RR rate coefficients and compared them with the CIE results of Mazzotta et al. (1998) for Mg, Si, S, Ar, Ca, Fe, and Ni. Our efforts here are just another step in what promises to be a long line of studies aimed at providing the astrophysics community with the most reliable CIE calculations currently possible.

The work here is motivated in specific by recent advances in our understanding of DR. With the development in the late 1980s of electron beam ion traps (EBITs) and heavy-ion storage rings

TABLE 1
PUBLISHED AUTOSTRUCTURE DR RATE COEFFICIENTS

Isoelectronic Sequence	Publication
H-like	Badnell (2006c)
He-like	Bautista & Badnell (2006)
Li-like	Colgan et al. (2004)
Be-like	Colgan et al. (2003)
B-like	Altun et al. (2004)
C-like	Zatsarinny et al. (2004a)
N-like	Mitnik & Badnell (2004)
O-like	Zatsarinny et al. (2003)
F-like	Zatsarinny et al. (2006)
Ne-like	Zatsarinny et al. (2004b); J. Fu et al. (in prep.)
Na-like	Altun et al. (2006)

NOTES.—Data have been published for all elements from He through Zn. These data were calculated using the techniques described in Badnell et al. (2003). The complete data set is provided via the weblink of Badnell (2006a).

combined with electron coolers, it has become possible to carry out detailed DR measurements for a wide range of systems (Müller & Wolf 1997; Schippers 1999; Beiersdorfer 2003). These results, in turn, have been used to test various state-of-the-art theoretical methods for calculating DR. Using these benchmarked methods, over the last few years a number of groups have systematically calculated DR for K- and L-shell ions and M-shell Na-like ions of various elements (Gu 2003b, 2004; Badnell et al. 2003; Badnell 2006a; see also Table 1). These groups have also recently calculated state-of-the-art RR rate coefficients for K- and L-shell ions and M-shell Na-like ions for a number of elements (Gu 2003a; Badnell 2006b, 2006d).

Using these new DR and RR results we have computed the CIE fraction abundances for the various ionization stages of all elements from H up to and including Zn. We present results for plasma temperatures from 10^4 to 10^9 K. The rest of this paper is organized as follows: In § 2 we review recent developments in our understanding of DR. Section 3 discusses recent improvements in the theoretical calculation of RR rate coefficients. In § 4 we discuss recent published unified DR + RR rate coefficients. Section 5 briefly discusses the status of the EII rate coefficients. Updating these data will be the subject of a future paper. In § 6 we give a short overview of the importance of CT in electron ionized plasmas. We will incorporate CT into future calculations. Section 7 outlines the equations relating ionization fractions to the rate coefficients and describes how we solve these equations. In § 8 we present our new CIE calculations and compare these results to the ionization balance results of Mazzotta et al. (1998) and to CIE calculations based on the data of Gu (2003b, 2003a, 2004). Section 9 discusses the results of our calculations and, in particular, how they differ from previous studies. Concluding remarks are given in § 10.

2. DIELECTRONIC RECOMBINATION (DR)

Dielectronic recombination (DR) is a two-step recombination process that begins when an electron collisionally excites a core electron of an ion and is simultaneously captured. The core electron excitation can be labeled $nl_j \rightarrow n'l'_{j'}$, where n is the principal quantum number, l is the orbital angular momentum, and j is the total angular momentum. We label the change in principal quantum number as $\Delta n = n' - n$. The energy of this intermediate system lies in the continuum and the complex may autoionize. The DR process is complete when the system emits a photon, reducing the total energy of the recombined system to below its ionization threshold. Conservation of energy requires that for DR to go forward $E_k = \Delta E - E_b$. Here E_k is the kinetic energy of the incident electron, ΔE the excitation energy of the initially bound electron in the presence of the captured electron, and E_b the binding energy released when the incident electron is captured onto the excited ion. Because ΔE and E_b are quantized, DR is a resonant process.

Badnell et al. (2003) have calculated the DR rate coefficients using the semirelativistic AUTOSTRUCTURE code (Badnell 1986) for the H- through Na-like isoelectronic sequences of all elements from He through to Zn (see Table 1; we use the convention here of identifying the recombination process by the initial charge state of the ion). These new DR data have been collected together and are available online (Badnell 2006a). In addition, some of the original data have been refitted so as to extend the validity of the fits to lower temperatures. Gu (2003b) has calculated DR rate coefficients using the relativistic FAC code for the H- through Ne-like isoelectronic sequences of Mg, Si, S, Ar, Ca, Fe, and Ni and for the Na-like sequence for Mg through Zn (Gu 2004). Both the calculations of Gu (2003b, 2004) and Badnell et al. (2003) were performed in the independent processes, isolated resonance approximation (Seaton & Storey 1976), using a distorted-wave representation. For the ions considered here, the low collision energies of the important DR resonances means that a fully relativistic treatment is not necessary. The methodology of the AUTOSTRUCTURE and FAC calculations is basically the same, with the differences coming mostly from the atomic structure.

In the temperature range where the fractional CIE abundance of an ion is greater than 0.01 (what we call here the CIE formation zone), we find the DR data of Badnell (2006a) and Gu (2003b, 2004) to be in good agreement except for Ne-like ions. The agreement is to within better than ~35% for Li-like Mg and ~25% for other Mg ions, ~25% for Si and S ions, ~20% for Ar and Ca ions, and ~15% for Fe and Ni ions.

For Ne-like ions the agreement is significantly poorer (Gu 2003b; Zatsarinny et al. 2004b; J. Fu et al. 2007, in preparation). Differences are seen of up to ~140% for Mg^{2+} and Si^{4+}, ~55% for S^{6+}, ~60% for Ar^{8+}, ~35% for Ca^{10+}, and ~15% for Fe^{16+} and Ni^{18+}. However, these differences occur at temperatures below the peak in the DR rate coefficient, where recombination is dominated by RR and DR is unimportant. A comparison of peak DR rate coefficients reveals differences of ~30% for Mg^{2+} and ~10% for the remaining six ions calculated by Gu (2003b).

In CIE, for K-shell ions of the elements considered here DR proceeds via $\Delta n \geq 1$ core excitations independent of the atomic number Z of the system. These have been well studied experimentally using EBITs and storage rings. State-of-the-art DR theory such as that of Badnell (2006a) and Gu (2003b) reproduce the experimental results with agreement on the order of ~20% (Müller 1995; Savin & Laming 2002).

For Li- to Na-like L- and M-shell ions of the elements considered here, at low Z DR proceeds primarily via $\Delta n = 0$ core excitations (except for Ne-like ions, which have no $\Delta n = 0$ channels). For intermediate Z, DR proceeds via a mix of $\Delta n = 0$ and 1 core excitation. At higher Z, DR proceeds primarily via $\Delta n = 1$ excitations. DR for all these ions is not as well understood as for K-shell systems.

Storage ring measurements of the L shell have been reviewed most recently by Schippers (1999) and Savin et al. (2006). Experimental work on M-shell Na-like systems is given in Linkemann et al. (1995), Müller (1999), and Fogle et al. (2003). For $\Delta n = 0$ DR, quite a number of laboratory measurements exist for Li- and Be-like ions. Significantly less work exists for B-, C-, N-, O-, F-, and Na-like ions. For C-, N-, and O-like ions, storage ring measurements exist for only a single ion in each sequence. For

TABLE 2
SOURCES OF DATA FOR THE AUTOSTRUCTURE-BASED CIE CALCULATIONS

Isoelectronic Sequence	DR Data Source	RR Data Source	EII Data Source
Bare	...	Badnell (2006d)	...
H-like	Badnell (2006c)	Badnell (2006d)	Mazzotta et al. (1998)[a]
He-like	Bautista & Badnell (2006)	Badnell (2006d)	Mazzotta et al. (1998)[a]
Li-like	Colgan et al. (2004)	Badnell (2006d)	Mazzotta et al. (1998)[a]
Be-like	Colgan et al. (2003)	Badnell (2006d)	Mazzotta et al. (1998)[a]
B-like	Altun et al. (2004)	Badnell (2006d)	Mazzotta et al. (1998)[a]
C-like	Zatsarinny et al. (2004a)	Badnell (2006d)	Mazzotta et al. (1998)[a]
N-like	Mitnik & Badnell (2004)	Badnell (2006d)	Mazzotta et al. (1998)[a]
O-like	Zatsarinny et al. (2003)	Badnell (2006d)	Mazzotta et al. (1998)[a]
F-like	Zatsarinny et al. (2006)	Badnell (2006d)	Mazzotta et al. (1998)[a]
Ne-like	Zatsarinny et al. (2004b); J. Fu et al. (in prep.)	Badnell (2006d)	Mazzotta et al. (1998)[a]
Na-like	Altun et al. (2006)	Badnell (2006d)	Mazzotta et al. (1998)[a]
Mg-like	Mazzotta et al. (1998)[a]	Mazzotta et al. (1998)[a]	Mazzotta et al. (1998)[a]
Al-like	Mazzotta et al. (1998)[a]	Mazzotta et al. (1998)[a]	Mazzotta et al. (1998)[a]
Si-like	Mazzotta et al. (1998)[a]	Mazzotta et al. (1998)[a]	Mazzotta et al. (1998)[a]
P-like	Mazzotta et al. (1998)[a]	Mazzotta et al. (1998)[a]	Mazzotta et al. (1998)[a]
S-like	Mazzotta et al. (1998)[a]	Mazzotta et al. (1998)[a]	Mazzotta et al. (1998)[a]
Cl-like	Mazzotta et al. (1998)[a]	Mazzotta et al. (1998)[a]	Mazzotta et al. (1998)[a]
Ar-like	Mazzotta et al. (1998)[a]	Mazzotta et al. (1998)[a]	Mazzotta et al. (1998)[a]
K-like	Mazzotta et al. (1998)[a]	Mazzotta et al. (1998)[a]	Mazzotta et al. (1998)[a]
Ca-like	Mazzotta et al. (1998)[a]	Mazzotta et al. (1998)[a]	Mazzotta et al. (1998)[a]
Sc-like	Mazzotta et al. (1998)[a]	Mazzotta et al. (1998)[a]	Mazzotta et al. (1998)[a]
Ti-like	Mazzotta et al. (1998)[a]	Mazzotta et al. (1998)[a]	Mazzotta et al. (1998)[a]
V-like	Mazzotta et al. (1998)[a]	Mazzotta et al. (1998)[a]	Mazzotta et al. (1998)[a]
Cr-like	Mazzotta et al. (1998)[a]	Mazzotta et al. (1998)[a]	Mazzotta et al. (1998)[a]
Mn-like	Mazzotta et al. (1998)[a]	Mazzotta et al. (1998)[a]	Mazzotta et al. (1998)[a]
Fe-like	Mazzotta et al. (1998)[a]	Mazzotta et al. (1998)[a]	Mazzotta et al. (1998)[a]
Co-like	Mazzotta et al. (1998)[a]	Mazzotta et al. (1998)[a]	Mazzotta et al. (1998)[a]
Ni-like	P. Mazzotta (2000, private communication)	P. Mazzotta (2000, private communication)	Mazzotta et al. (1998)[a]
Cu-like	P. Mazzotta (2000, private communication)	P. Mazzotta (2000, private communication)	P. Mazzotta (2000, private communication)
Zn-like	...	...	P. Mazzotta (2000, private communication)

NOTES.—These are the data used to produce the CIE results given in Fig. Set 2 and Table 4. The AUTOSTRUCTURE DR data (Badnell 2006a) and RR data (Badnell 2006b) are also available online.

[a] The data from Mazzotta et al. (1998) is replaced by P. Mazzotta (2000, private communication) for the elements Cu and Zn.

the B-, F-, and Na-like ions, they exist for only two ions in each sequence. The situation for $\Delta n = 1$ DR is even spottier. Results have been published for some Li-, Be-, O-, F-, and Na-like ions. For the O-, F-, and Na-like ions, measurements exist for only one ion in each sequence. We are unaware of any published $\Delta n = 1$ measurements for ions in the B-, C-, N-, or Ne-like isoelectronic sequences. Clearly, additional benchmark laboratory work is called for.

To summarize the comparison between state-of-the-art theory and experiment for the above L- and M-shell isoelectronic sequences, for $\Delta n = 0$ DR at collision energies $\gtrsim 1$–3 eV and for $\Delta n = 1$ DR, agreement with the stronger DR resonances is typically better than 35%. Problems arise, however, with $\Delta n = 0$ DR for collision energies below $\lesssim 1$–3 eV, where modern theory has difficulty reliably calculating DR resonance energies. These differences translate directly into an uncertainty in the DR rate coefficient for $T_e \lesssim 10{,}000$–$35{,}000$ K. There is no clear Z dependence scaling for this energy or temperature limit. For example, Be-like C^{2+} (Fogle et al. 2005), B-like Ar^{13+} (DeWitt et al. 1996), and C-like Fe^{20+} (Savin et al. 2003) all show discrepancies between theory and experiment for energies below ~ 3 eV. On the other hand, O-like Fe^{18+}, F-like Fe^{17+}, and Na-like Ni^{17+} all show good agreement between theoretical and experimental resonance energies down to 0.1 eV (Savin et al. 1997, 1999; Fogle et al. 2003). The 1–3 eV limit given above is more a function of the Rydberg level into which the incident electron is captured. For high levels, correlation effects are unimportant and theory can reliably calculate the DR resonance energies and strengths and hence reliable DR rate coefficients. But for low levels, this is not the case.

The reliability of DR rate coefficients for $T_e \lesssim 35{,}000$ K must be evaluated on a case-by-case basis. Theoretical calculations can be used as an evaluation guide by determining which Rydberg levels are important below 3 eV. But laboratory benchmark measurements are also needed. Fortunately in CIE, only singly and doubly charged ions form in significant abundances at these temperatures (based on our fractional abundance calculations below). So any theoretical uncertainties will affect mostly DR data only for these ions. In a future work we will investigate theoretically for which ions this is most likely to be an issue.

Below 25,000 K, CT with atomic H is also important, as is discussed in § 6. Since we do not include CT in our CIE calculations here, we have also chosen not to include what little experimentally derived DR data for singly and doubly charged ions exist. Both CT and any published experimental DR results will be included in future work.

For ionization stages not included in the state-of-the-art calculations of Badnell (2006a) and Gu (2003b, 2004), we use the DR rate coefficients recommended by Mazzotta et al. (1998) for elements up to and including Ni and those recommended by P. Mazzotta (2000, private communication) for Cu and Zn. These older data come from a variety of sources and are typically less

TABLE 3
Sources of Data Used in the FAC-based CIE Calculations

Isoelectronic Sequence	DR Data Source	RR Data Source	EII Data Source
Bare	...	Gu (2003a)	...
H-like	Gu (2003b)	Gu (2003a)	Mazzotta et al. (1998)
He-like	Gu (2003b)	Gu (2003a)	Mazzotta et al. (1998)
Li-like	Gu (2003b)	Gu (2003a)	Mazzotta et al. (1998)
Be-like	Gu (2003b)	Gu (2003a)	Mazzotta et al. (1998)
B-like	Gu (2003b)	Gu (2003a)	Mazzotta et al. (1998)
C-like	Gu (2003b)	Gu (2003a)	Mazzotta et al. (1998)
N-like	Gu (2003b)	Gu (2003a)	Mazzotta et al. (1998)
O-like	Gu (2003b)	Gu (2003a)	Mazzotta et al. (1998)
F-like	Gu (2003b)	Gu (2003a)	Mazzotta et al. (1998)
Ne-like	Gu (2003b)	Mazzotta et al. (1998)	Mazzotta et al. (1998)
Na-like	Gu (2004)	Mazzotta et al. (1998)	Mazzotta et al. (1998)
Mg-like	Mazzotta et al. (1998)	Mazzotta et al. (1998)	Mazzotta et al. (1998)
Al-like	Mazzotta et al. (1998)	Mazzotta et al. (1998)	Mazzotta et al. (1998)
Si-like	Mazzotta et al. (1998)	Mazzotta et al. (1998)	Mazzotta et al. (1998)
P-like	Mazzotta et al. (1998)	Mazzotta et al. (1998)	Mazzotta et al. (1998)
S-like	Mazzotta et al. (1998)	Mazzotta et al. (1998)	Mazzotta et al. (1998)
Cl-like	Mazzotta et al. (1998)	Mazzotta et al. (1998)	Mazzotta et al. (1998)
Ar-like	Mazzotta et al. (1998)	Mazzotta et al. (1998)	Mazzotta et al. (1998)
K-like	Mazzotta et al. (1998)	Mazzotta et al. (1998)	Mazzotta et al. (1998)
Ca-like	Mazzotta et al. (1998)	Mazzotta et al. (1998)	Mazzotta et al. (1998)
Sc-like	Mazzotta et al. (1998)	Mazzotta et al. (1998)	Mazzotta et al. (1998)
Ti-like	Mazzotta et al. (1998)	Mazzotta et al. (1998)	Mazzotta et al. (1998)
V-like	Mazzotta et al. (1998)	Mazzotta et al. (1998)	Mazzotta et al. (1998)
Cr-like	Mazzotta et al. (1998)	Mazzotta et al. (1998)	Mazzotta et al. (1998)
Mn-like	Mazzotta et al. (1998)	Mazzotta et al. (1998)	Mazzotta et al. (1998)
Fe-like	Mazzotta et al. (1998)	Mazzotta et al. (1998)	Mazzotta et al. (1998)
Co-like	Mazzotta et al. (1998)	Mazzotta et al. (1998)	Mazzotta et al. (1998)
Ni-like	...	...	Mazzotta et al. (1998)

Note.—These are the data used to produce the CIE results given in Fig. Set 3 and Table 5.

reliable than more modern results. The sources of DR data used in our CIE calculations are listed in Tables 2 and 3.

3. RADIATIVE RECOMBINATION (RR)

Radiative recombination (RR) is a one-step recombination process that occurs when a free electron is captured by an ion. Energy and momentum are conserved in the process by the simultaneous emission of a photon. Quantum mechanically, DR and RR are indistinguishable processes that interfere with each other. Pindzola et al. (1992) have shown that this interference is a very small effect and can safely be neglected in most cases. This gives the independent processes approximation whereby DR and RR can be considered separately. At high temperatures RR is unimportant in comparison to DR so relativistic effects of the colliding electron need not be considered.

Gu (2003a) has calculated RR rate coefficients for ions of Mg, Si, S, Ar, Ca, Fe, and Ni for bare through F-like ions using FAC. Badnell (2006d) has calculated RR rate coefficients for all elements from H through to Zn for the bare through Na-like isoelectronic sequences using AUTOSTRUCTURE. These AUTOSTRUCTURE data are available online (Badnell 2006b).

The AUTOSTRUCTURE results agree with those of Verner & Ferland (1996) to better than 5% in the CIE zone. The results of Gu (2003a) and Badnell (2006b) agree to within ~10% in the CIE formation zone, except for the H-like ions of Ar, Ca, Fe, and Ni. For these ions, the FAC rate coefficients of Gu (2003a) are systematically smaller than the AUTOSTRUCTURE data of Badnell (2006b). The FAC results show negligible differences with the AUTOSTRUCTURE data at the low-temperature limit of the CIE formation zone, but these differences rise to ~20% at the high-temperature limit. For these four H-like ions in this temperature range, RR dominates over DR. It should be noted, however, that in CIE the total electron-ion recombination rate is generally dominated by DR rather than RR. So uncertainties in RR data typically have less of an effect than those of DR data for fractional abundance calculations of most ions in CIE.

For ionization stages not included in the calculations of Badnell (2006b) and Gu (2003a), we use the RR rate coefficients recommended by Mazzotta et al. (1998) for elements up to and including Ni and those recommended by P. Mazzotta (2000, private communication) for Cu and Zn. The sources of RR data used in our CIE calculations are listed in Tables 2 and 3.

4. UNIFIED DR + RR CALCULATIONS

Nahar & Pradhan (1997) have presented theoretical unified electron-ion recombination rate coefficients (i.e., DR + RR). The currently available data from these works include all ionization stages of C (Nahar & Pradhan 1997; Nahar et al. 2000), N (Nahar & Pradhan 1997; Nahar 2006), and O (Nahar 1999; Nahar & Pradhan 2006); the bare, H-, and He-like ions of F (Nahar 2006), Ne (Nahar & Pradhan 2006), Fe (Nahar et al. 2001), and Ni (Nahar 2005b); and B-like Ar (Nahar 2005a). We have compared these results with the summed DR + RR results from the AUTOSTRUCTURE calculations (Badnell 2006a, 2006b).

In the CIE formation zone, agreement is within 20% for C^{q+} ($q = 1, 2, 4,$ and 5), N^{q+} ($q = 3, 4,$ and 6), O^{q+} ($q = 1, 2, 4,$ and 5), F^{q+} ($q = 7$ and 8), Ne^{q+} ($q = 8$ and 9), Ar^{13+}, and Ni^{q+} ($q = 26$ and 27). It is within 30% for N^{q+} ($q = 2$ and 5), O^{q+} ($q = 3$ and 7), and Fe^{25+}. For the bare ions, where there is no DR contribution to the recombination rate coefficient, agreement is to within a few percent. The only ions that have differences greater than ~30% are C^{3+}, N^{1+}, and Fe^{24+}.

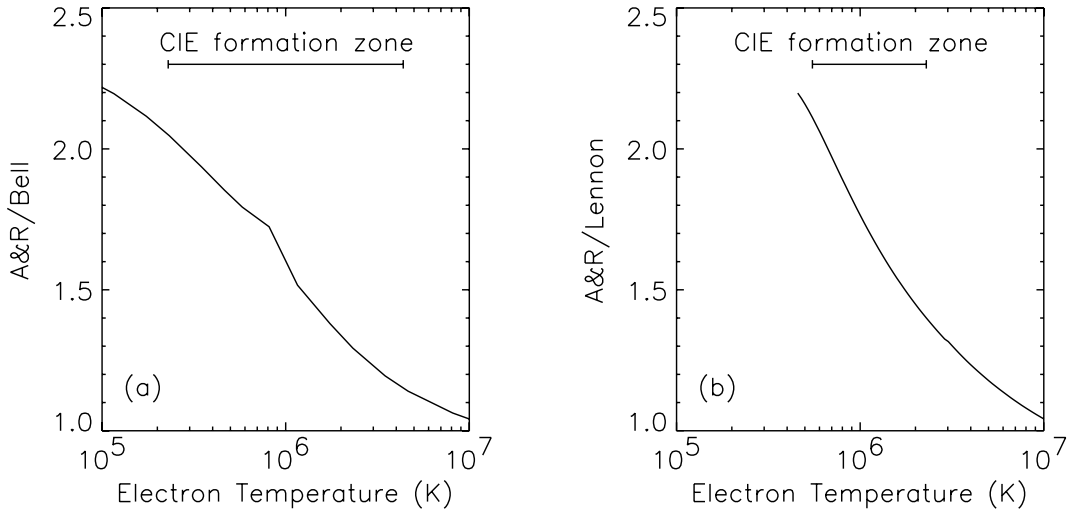

FIG. 1.—Ratio of the recommended EII rate coefficients of Arnaud & Rothenflug (1985, A&R) relative to the recommended data of (*a*) Bell et al. (1983) for He-like O^{6+} and (*b*) Lennon et al. (1988) for O-like S^{8+}. The horizontal bars show the temperature range over which these ions form in CIE.

For the C^{3+} ion the difference is ~35%. However, the results of Nahar & Pradhan (2003) were calculated using LS-coupling for this ion and are in good agreement (better than 18%) with the LS-coupling results of AUTOSTRUCTURE (unpublished). The CIE peak DR rate coefficient for C^{3+} is enhanced by 30% when using intermediate coupling. Using such a coupling scheme, Pradhan et al. (2001) have carried out Breit-Pauli *R*-matrix recombination calculations for C^{3+} so as to compare with experiment but, to our knowledge, no Maxwellian rate coefficient has been made publicly available. We expect their data would be in better agreement with the summed DR + RR AUTOSTRUCTURE results.

The disagreement in the N^{1+} rate coefficient is largest at the low-temperature end of the CIE range (up to 60% at 10^4 K), where the $2s^2 2p^4\ ^2D$ DR resonance dominates. The source of this difference may lie in the energy used for this resonance. The AUTOSTRUCTURE results are in close agreement with those of Nussbaumer & Storey (1983). Both use the observed position of this resonance. The difference is unlikely to be due to fine structure as DR via fine structure core excitations does not become important for this ion until below 10^3 K, well outside of the CIE range.

For Fe^{24+} the calculations of Nahar et al. (2001) track the RR calculations of Badnell (2006b) closely; but above 10^7 K, where the DR contribution to the total recombination rate coefficient becomes important, we find the Nahar et al. (2001) results to be around 45% larger than the summed (DR + RR) AUTOSTRUCTURE results. The source of this difference is unclear, but Gorczyca & Badnell (1997) have shown that DR resonance interference for Fe^{24+} is negligible so this is unlikely to be the cause. The AUTOSTRUCTURE RR rate coefficients differ by no more than 5% from those of Verner & Ferland (1996) over the entire CIE temperature range, while the DR rate coefficients differ by no more than 10% from those of Gu (2003b) over this range.

5. ELECTRON IMPACT IONIZATION

Electron impact ionization (EII) can occur through either direct ionization or indirect processes such as excitation-autoionization (EA) and resonant-excitation double autoionization (REDA). Direct ionization is a nonresonant process. Direct outer-shell ionization typically changes the charge of the initial atom or ion by one. Direct inner-shell ionization produces a hole in the shell and a free electron. As the ion stabilizes to fill the hole, up to six Auger electrons can be emitted (Kaastra & Mewe 1993; Gorczyca et al. 2003). EA occurs when an incident electron collisionally excites an ion to a state that then decays by autoionization rather than radiative decay. REDA begins when the incident electron is captured by an ion and simultaneously excites a bound electron of the ion. REDA is complete when this recombined system autoionizes by emission of two electrons. Thus, the initial ion has moved one higher in charge state. For ions with certain electron configurations, such as those with one or two valence electrons, EA and, to a lesser extent, REDA can significantly enhance ionization cross sections compared to the direct ionization contribution (e.g., Linkemann et al. 1995).

The most recent set of CIE calculations (Mazzotta et al. 1998) used the recommended data of Arnaud & Rothenflug (1985) and Arnaud & Raymond (1992). These EII data are derived from a combination of laboratory measurements and theoretical calculations. Other workers have derived recommended rate coefficients using essentially the same measurements and calculations (Bell et al. 1983; Pindzola et al. 1987; Lennon et al. 1988). All of these recommended EII rate coefficients have been compared by Kato et al. (1991). Taking into account known typographical errors in the recommended EII data, Kato et al. found differences between the various recommended data of up to a factor of 2–3 for many ions (see, e.g., Fig. 1). These differences are not in the fits to the data but in the derived recommended data. This is somewhat surprising considering that the recommended rate coefficients are basically all derived from the same experimental and theoretical data.

In the present paper we use the EII rate coefficients for all ionization states of H through Ni from Mazzotta et al. (1998). This means that any and all subsequent differences between our new fractional abundances and those of Mazzotta et al. (1998) can be attributed to the changes in the recombination rate coefficients used (barring any computational or round-off errors). For Cu and Zn we use the recommended rate coefficients of P. Mazzotta (2000, private communication) based on extrapolation of the fitting parameters from other elements. The sources of EII data used in our CIE calculations are listed in Tables 2 and 3.

Mazzitelli & Mattioli (2002) have also published EII rate coefficients for Cu and Zn, but they differ from the P. Mazzotta (2000, private communication) data only for the lowest three ionization stages of Cu and the lowest four ionization stages of Zn. For these seven ions, however, the data of Mazzitelli & Mattioli do not offer any significant improvement on the Mazzotta data as the Mazzitelli & Mattioli data are taken from sources that predate the Mazzotta work (Lotz 1968; Higgins et al. 1989). Since the intention of our paper is to investigate the effects of updated

recombination rate coefficients, and for consistency with the comparisons for other elements, we use the Mazzotta EII rate coefficients for Cu and Zn.

A fully relativistic treatment of electron impact ionization is often required for highly ionized species, which require much higher incident electron energies to ionize. For example, the ionization of near fully stripped U is highly dependent on the relativistic treatment (Pindzola & Buie 1998), particularly for *s*-orbitals. On the other hand, Loch et al. (2005) found a semirelativistic treatment of W^{9+} at 5 keV to be in close agreement with experiment. The same study showed that a fully relativistic treatment was not required until W^{64+}. For all lower tungsten ion stages, a semirelativistic treatment produced good results. Since we do not consider elements above Zn in this work, theoretical calculations using a fully relativistic treatment are not needed for the present CIE modeling. A semirelativistic approach should be able to produce accurate results for the higher charge states of the ions in this work.

It is not clear, however, that reliable semirelativistic calculations exist among the currently used recommended EII rate coefficients. We have already mentioned the problems noted by Kato et al. (1991). In addition, much of the data are based on experiments with unknown metastable fractions. The resulting rate coefficients represent some average over a distribution of ground state and metastable populations. This is often an acceptable approximation for magnetically confined fusion plasmas, which can have high metastable ion content. But this is generally unsuitable for astrophysical plasmas of the type considered here where the ions are in their ground state. Finally, the recommended EII data currently used by the astrophysics community has not undergone any significant revision or laboratory benchmarking since around 1990. It is clear that an updating of the EII database is sorely needed.

6. CHARGE TRANSFER

Charge transfer (CT), also known as charge exchange or electron capture, is the reaction whereby an ion captures an electron from a donor atom. For plasmas of cosmic abundances, this is typically atomic hydrogen but, in some instances, can be neutral helium or other neutral atoms.

The importance of CT with H can be readily demonstrated (e.g., Kingdon & Ferland 1996). In CIE, CT is most important for near-neutral systems, up to 4 times ionized (Arnaud & Rothenflug 1985). Using the data of Badnell (2006a, 2006b) and Gu (2003b, 2003a, 2004) for these ions, a typical rate coefficient for DR + RR is on the order of $\alpha_{\mathrm{DR+RR}} \approx 10^{-11}$ cm^3 s^{-1}. A large CT rate coefficient is on the order of $\alpha_{\mathrm{CT}} \approx 10^{-9}$ cm^3 s^{-1} (Kingdon & Ferland 1996). Using these values one finds that, for a given ion, the ratio of the CT to DR + RR rates is given by

$$\frac{R_{\mathrm{CT}}}{R_{\mathrm{DR+RR}}} = \frac{\alpha_{\mathrm{CT}} n_{\mathrm{H}^0}}{\alpha_{\mathrm{DR+RR}} n_e} \approx 10^2 \frac{n_{\mathrm{H}^0}}{n_e} \approx 10^2 \frac{n_{\mathrm{H}^0}}{n_{\mathrm{H}^+}}, \qquad (1)$$

where n_{H^0} is the neutral H density, n_e is the electron density, and n_{H^+} is the H^+ density. The last approximation makes use of $n_{\mathrm{e}} \approx n_{\mathrm{H}^+}$ for plasmas with cosmic abundances. As one can see, the CT rate will be equal to or greater than the DR + RR rate provided that $n_{\mathrm{H}^0}/n_{\mathrm{H}^+} \gtrsim 0.01$. This inequality holds for electron temperatures $T_{\mathrm{e}} \lesssim 25{,}000$ K (see Fig. 2.1 and Table 4).

Arnaud & Rothenflug (1985) have investigated the effects of CT on CIE and found the process to be important for a number of ions of astrophysical abundance. Those they list for CT with H are He^{q+} ($q = 1$–2); C^{q+}, N^{q+}, O^{q+}, and S^{q+} ($q = 1$–4); and Ne^{q+}, Mg^{q+}, Si^{q+}, and Ar^{q+} ($q = 2$–4). For CT with He, they list C^{q+}, N^{q+}, O^{q+}, Ne^{q+}, and Ar^{q+} ($q = 2$–4); and Mg^{q+}, Si^{q+}, and S^{q+} ($q = 3$–4). The reverse reaction, CT ionization with H^+, was also found to be comparable to EII for O^{0+}, Si^{0+}, S^{0+}, Mg^{1+}, and Si^{1+}. CT ionization with He^{1+} was found to be important for C^{1+}, N^{1+}, Si^{1+}, Si^{2+}, S^{1+}, S^{2+}, and Ar^{1+}. Many of the ions listed in this paragraph form at temperatures above 25,000 K. This points out the crudeness of our above back-of-the-envelope estimate. Clearly, a more detailed study is needed using data more modern than that used by Arnaud & Rothenflug (1985).

We will incorporate CT into our results in a future work. Until then, our CIE results at low temperatures should be used with caution, particularly for temperatures $\lesssim$25,000 K, where neutral H is abundant.

7. COLLISIONAL IONIZATION EQUILIBRIUM CALCULATION

We work in the coronal approximation where each ionization stage is represented by its ground population only, i.e., metastable populations are assumed zero. We neglect the effects of any radiation field, three-body processes, charge transfer, and electron density effects.

The total abundance of element X is given by

$$N_{\mathrm{tot}} = \sum_{i=0}^{Z} N^i, \qquad (2)$$

where N^q is the population of ion X^{q+}, q is the charge, and Z is the atomic number of X. The fractional abundance of charge state q is then given by

$$f^q = \frac{N^q}{N_{\mathrm{tot}}}. \qquad (3)$$

This leads naturally to the normalization

$$\sum_{i=0}^{Z} f^i = 1. \qquad (4)$$

For a given system, the nearby charge stages are linked by the total recombination and ionization coefficients. For the present calculations, the total recombination coefficient is the sum of the DR and RR rate coefficients. The total ionization rate coefficient is simply the EII rate coefficient. For the more general CIE case, one would need also to account for CT recombination and ionization. For recombination from stage q to $q-1$, we write the total recombination rate coefficient as $\alpha_{\mathrm{tot}}^{q\rightarrow q-1}$ and, for ionization from stage q to stage $q+1$, we write the total ionization rate coefficient as $S_{\mathrm{tot}}^{q\rightarrow q+1}$. Here we only consider changes in charge state of $\Delta q = \pm 1$, as has commonly be done in the past for CIE calculations. Changes of $\Delta q > \pm 1$ will be considered in future work.

In coronal equilibrium, the populations are unchanging in time and can be written in matrix form as

$$N_{\mathrm{tot}} \frac{d}{dt} \begin{bmatrix} f^0 \\ f^1 \\ \vdots \end{bmatrix} = \begin{bmatrix} 0 \\ 0 \\ \vdots \end{bmatrix}. \qquad (5)$$

In terms of α_{tot}, S_{tot}, and electron density, n_e, the populations can be written as

$$N_{\mathrm{tot}} n_e \begin{bmatrix} -S_{\mathrm{tot}}^{0\rightarrow 1} & \alpha_{\mathrm{tot}}^{1\rightarrow 0} & 0 \\ S_{\mathrm{tot}}^{0\rightarrow 1} & -\alpha_{\mathrm{tot}}^{1\rightarrow 0} - S_{\mathrm{tot}}^{1\rightarrow 2} & \alpha_{\mathrm{tot}}^{2\rightarrow 1} \\ 0 & S_{\mathrm{tot}}^{1\rightarrow 2} & \ddots \end{bmatrix} \begin{bmatrix} f^0 \\ f^1 \\ \vdots \end{bmatrix} = \begin{bmatrix} 0 \\ 0 \\ \vdots \end{bmatrix}. \qquad (6)$$

TABLE 4

SAMPLE CIE FRACTIONAL ABUNDANCES (AUTOSTRUCTURE-BASED RESULTS): IRON

log (T)	Fe^{0+}	Fe^{1+}	Fe^{2+}	Fe^{3+}	Fe^{4+}	Fe^{5+}	Fe^{6+}	Fe^{7+}	Fe^{8+}	Fe^{9+}	Fe^{10+}	Fe^{11+}	Fe^{12+}	Fe^{13+}
4.00	0.916	0.056	4.006	15.000	15.000	15.000	15.000	15.000	15.000	15.000	15.000	15.000	15.000	15.000
4.10	1.450	0.019	2.165	15.000	15.000	15.000	15.000	15.000	15.000	15.000	15.000	15.000	15.000	15.000
4.20	1.981	0.085	0.776	8.101	15.000	15.000	15.000	15.000	15.000	15.000	15.000	15.000	15.000	15.000
4.30	2.883	0.589	0.130	5.069	15.000	15.000	15.000	15.000	15.000	15.000	15.000	15.000	15.000	15.000
4.40	3.933	1.291	0.023	3.046	10.640	15.000	15.000	15.000	15.000	15.000	15.000	15.000	15.000	15.000
4.50	4.698	1.747	0.021	1.520	6.727	15.000	15.000	15.000	15.000	15.000	15.000	15.000	15.000	15.000
4.60	5.371	2.145	0.158	0.527	3.813	10.373	15.000	15.000	15.000	15.000	15.000	15.000	15.000	15.000
4.70	6.163	2.688	0.507	0.170	1.969	6.405	13.158	15.000	15.000	15.000	15.000	15.000	15.000	15.000
4.80	6.947	3.245	0.897	0.127	0.898	3.638	8.368	15.000	15.000	15.000	15.000	15.000	15.000	15.000
4.90	7.784	3.872	1.369	0.279	0.380	1.843	5.095	10.166	15.000	15.000	15.000	15.000	15.000	15.000
5.00	8.732	4.623	1.972	0.610	0.224	0.835	3.049	6.479	11.453	15.000	15.000	15.000	15.000	15.000
5.10	9.801	5.504	2.709	1.101	0.322	0.370	1.808	4.080	7.575	15.000	15.000	15.000	15.000	15.000
5.20	10.947	6.470	3.532	1.695	0.581	0.208	1.023	2.491	4.934	12.007	15.000	15.000	15.000	15.000
5.30	12.164	7.514	4.430	2.376	0.969	0.250	0.544	1.405	3.056	8.535	14.671	15.000	15.000	15.000
5.40	13.504	8.685	5.453	3.190	1.522	0.503	0.350	0.720	1.741	5.916	10.608	15.000	15.000	15.000
5.50	15.000	10.023	6.640	4.174	2.268	0.984	0.441	0.395	0.901	4.005	7.517	11.373	15.000	15.000
5.60	15.000	11.506	7.968	5.304	3.179	1.655	0.766	0.361	0.434	2.658	5.206	8.100	11.438	15.000
5.70	15.000	13.060	9.365	6.506	4.176	2.431	1.232	0.510	0.215	1.715	3.476	5.569	8.043	11.515
5.80	15.000	14.627	10.774	7.723	5.199	3.248	1.767	0.762	0.147	1.049	2.166	3.587	5.346	7.950
5.90	15.000	15.000	12.211	8.970	6.260	4.116	2.377	1.113	0.216	0.620	1.208	2.061	3.221	5.102
6.00	15.000	15.000	13.783	10.357	7.468	5.140	3.164	1.662	0.512	0.495	0.640	1.010	1.664	2.936
6.10	15.000	15.000	15.000	12.049	8.988	6.482	4.288	2.565	1.183	0.805	0.574	0.531	0.751	1.502
6.20	15.000	15.000	15.000	14.088	10.860	8.184	5.788	3.856	2.260	1.566	1.007	0.609	0.451	0.752
6.30	15.000	15.000	15.000	15.000	13.129	10.287	7.704	5.575	3.779	2.805	1.955	1.247	0.755	0.663
6.40	15.000	15.000	15.000	15.000	15.000	12.798	10.040	7.723	5.738	4.509	3.398	2.418	1.627	1.187
6.50	15.000	15.000	15.000	15.000	15.000	15.000	12.409	9.912	7.748	6.287	4.937	3.713	2.653	1.904
6.60	15.000	15.000	15.000	15.000	15.000	15.000	14.647	11.978	9.642	7.966	6.397	4.952	3.648	2.622
6.70	15.000	15.000	15.000	15.000	15.000	15.000	15.000	13.932	11.432	9.557	7.784	6.137	4.610	3.335
6.80	15.000	15.000	15.000	15.000	15.000	15.000	15.000	15.000	13.182	11.119	9.156	7.322	5.590	4.089
6.90	15.000	15.000	15.000	15.000	15.000	15.000	15.000	15.000	14.983	12.744	10.602	8.592	6.670	4.964
7.00	15.000	15.000	15.000	15.000	15.000	15.000	15.000	15.000	15.000	14.547	12.236	10.061	7.963	6.068
7.10	15.000	15.000	15.000	15.000	15.000	15.000	15.000	15.000	15.000	15.000	14.187	11.857	9.593	7.524
7.20	15.000	15.000	15.000	15.000	15.000	15.000	15.000	15.000	15.000	15.000	15.000	13.991	11.571	9.339
7.30	15.000	15.000	15.000	15.000	15.000	15.000	15.000	15.000	15.000	15.000	15.000	15.000	13.677	11.288
7.40	15.000	15.000	15.000	15.000	15.000	15.000	15.000	15.000	15.000	15.000	15.000	15.000	15.000	13.198
7.50	15.000	15.000	15.000	15.000	15.000	15.000	15.000	15.000	15.000	15.000	15.000	15.000	15.000	15.000
7.60	15.000	15.000	15.000	15.000	15.000	15.000	15.000	15.000	15.000	15.000	15.000	15.000	15.000	15.000
7.70	15.000	15.000	15.000	15.000	15.000	15.000	15.000	15.000	15.000	15.000	15.000	15.000	15.000	15.000
7.80	15.000	15.000	15.000	15.000	15.000	15.000	15.000	15.000	15.000	15.000	15.000	15.000	15.000	15.000
7.90	15.000	15.000	15.000	15.000	15.000	15.000	15.000	15.000	15.000	15.000	15.000	15.000	15.000	15.000
8.00	15.000	15.000	15.000	15.000	15.000	15.000	15.000	15.000	15.000	15.000	15.000	15.000	15.000	15.000
8.10	15.000	15.000	15.000	15.000	15.000	15.000	15.000	15.000	15.000	15.000	15.000	15.000	15.000	15.000
8.20	15.000	15.000	15.000	15.000	15.000	15.000	15.000	15.000	15.000	15.000	15.000	15.000	15.000	15.000
8.30	15.000	15.000	15.000	15.000	15.000	15.000	15.000	15.000	15.000	15.000	15.000	15.000	15.000	15.000
8.40	15.000	15.000	15.000	15.000	15.000	15.000	15.000	15.000	15.000	15.000	15.000	15.000	15.000	15.000
8.50	15.000	15.000	15.000	15.000	15.000	15.000	15.000	15.000	15.000	15.000	15.000	15.000	15.000	15.000
8.60	15.000	15.000	15.000	15.000	15.000	15.000	15.000	15.000	15.000	15.000	15.000	15.000	15.000	15.000
8.70	15.000	15.000	15.000	15.000	15.000	15.000	15.000	15.000	15.000	15.000	15.000	15.000	15.000	15.000
8.80	15.000	15.000	15.000	15.000	15.000	15.000	15.000	15.000	15.000	15.000	15.000	15.000	15.000	15.000
8.90	15.000	15.000	15.000	15.000	15.000	15.000	15.000	15.000	15.000	15.000	15.000	15.000	15.000	15.000
9.00	15.000	15.000	15.000	15.000	15.000	15.000	15.000	15.000	15.000	15.000	15.000	15.000	15.000	15.000

log (T)	Fe^{14+}	Fe^{15+}	Fe^{16+}	Fe^{17+}	Fe^{18+}	Fe^{19+}	Fe^{20+}	Fe^{21+}	Fe^{22+}	Fe^{23+}	Fe^{24+}	Fe^{25+}	Fe^{26+}
4.00	15.000	15.000	15.000	15.000	15.000	15.000	15.000	15.000	15.000	15.000	15.000	15.000	15.000
4.10	15.000	15.000	15.000	15.000	15.000	15.000	15.000	15.000	15.000	15.000	15.000	15.000	15.000
4.20	15.000	15.000	15.000	15.000	15.000	15.000	15.000	15.000	15.000	15.000	15.000	15.000	15.000
4.30	15.000	15.000	15.000	15.000	15.000	15.000	15.000	15.000	15.000	15.000	15.000	15.000	15.000
4.40	15.000	15.000	15.000	15.000	15.000	15.000	15.000	15.000	15.000	15.000	15.000	15.000	15.000
4.50	15.000	15.000	15.000	15.000	15.000	15.000	15.000	15.000	15.000	15.000	15.000	15.000	15.000
4.60	15.000	15.000	15.000	15.000	15.000	15.000	15.000	15.000	15.000	15.000	15.000	15.000	15.000
4.70	15.000	15.000	15.000	15.000	15.000	15.000	15.000	15.000	15.000	15.000	15.000	15.000	15.000
4.80	15.000	15.000	15.000	15.000	15.000	15.000	15.000	15.000	15.000	15.000	15.000	15.000	15.000
4.90	15.000	15.000	15.000	15.000	15.000	15.000	15.000	15.000	15.000	15.000	15.000	15.000	15.000
5.00	15.000	15.000	15.000	15.000	15.000	15.000	15.000	15.000	15.000	15.000	15.000	15.000	15.000
5.10	15.000	15.000	15.000	15.000	15.000	15.000	15.000	15.000	15.000	15.000	15.000	15.000	15.000

TABLE 4—*Continued*

log (T)	Fe^{14+}	Fe^{15+}	Fe^{16+}	Fe^{17+}	Fe^{18+}	Fe^{19+}	Fe^{20+}	Fe^{21+}	Fe^{22+}	Fe^{23+}	Fe^{24+}	Fe^{25+}	Fe^{26+}
5.20.....	15.000	15.000	15.000	15.000	15.000	15.000	15.000	15.000	15.000	15.000	15.000	15.000	15.000
5.30.....	15.000	15.000	15.000	15.000	15.000	15.000	15.000	15.000	15.000	15.000	15.000	15.000	15.000
5.40.....	15.000	15.000	15.000	15.000	15.000	15.000	15.000	15.000	15.000	15.000	15.000	15.000	15.000
5.50.....	15.000	15.000	15.000	15.000	15.000	15.000	15.000	15.000	15.000	15.000	15.000	15.000	15.000
5.60.....	15.000	15.000	15.000	15.000	15.000	15.000	15.000	15.000	15.000	15.000	15.000	15.000	15.000
5.70.....	15.000	15.000	15.000	15.000	15.000	15.000	15.000	15.000	15.000	15.000	15.000	15.000	15.000
5.80.....	10.923	14.448	15.000	15.000	15.000	15.000	15.000	15.000	15.000	15.000	15.000	15.000	15.000
5.90.....	7.281	9.903	11.968	15.000	15.000	15.000	15.000	15.000	15.000	15.000	15.000	15.000	15.000
6.00.....	4.439	6.292	7.615	13.224	15.000	15.000	15.000	15.000	15.000	15.000	15.000	15.000	15.000
6.10.....	2.421	3.616	4.383	8.649	13.594	15.000	15.000	15.000	15.000	15.000	15.000	15.000	15.000
6.20.....	1.163	1.797	2.162	5.382	9.157	13.546	15.000	15.000	15.000	15.000	15.000	15.000	15.000
6.30.....	0.628	0.791	0.856	3.263	6.119	9.480	13.285	15.000	15.000	15.000	15.000	15.000	15.000
6.40.....	0.762	0.538	0.360	2.127	4.259	6.807	9.712	13.059	15.000	15.000	15.000	15.000	15.000
6.50.....	1.136	0.593	0.207	1.457	3.011	4.913	7.099	9.659	12.492	15.000	15.000	15.000	15.000
6.60.....	1.553	0.744	0.169	0.991	2.072	3.452	5.059	6.984	9.114	11.503	13.946	15.000	15.000
6.70.....	1.998	0.962	0.210	0.669	1.353	2.301	3.433	4.839	6.394	8.176	9.973	15.000	15.000
6.80.....	2.514	1.276	0.358	0.499	0.844	1.426	2.159	3.133	4.212	5.493	6.755	14.535	15.000
6.90.....	3.174	1.754	0.675	0.536	0.582	0.847	1.238	1.846	2.524	3.386	4.202	10.412	15.000
7.00.....	4.084	2.494	1.259	0.868	0.648	0.633	0.726	1.015	1.350	1.855	2.298	7.239	12.876
7.10.....	5.361	3.611	2.225	1.604	1.144	0.877	0.704	0.714	0.751	0.948	1.080	4.990	9.549
7.20.....	7.012	5.109	3.576	2.743	2.062	1.567	1.155	0.914	0.687	0.616	0.492	3.563	7.242
7.30.....	8.807	6.758	5.080	4.050	3.166	2.460	1.829	1.360	0.900	0.593	0.256	2.643	5.600
7.40.....	10.571	8.379	6.559	5.345	4.270	3.369	2.536	1.858	1.187	0.673	0.158	1.983	4.342
7.50.....	12.255	9.926	7.967	6.579	5.325	4.241	3.220	2.349	1.487	0.785	0.117	1.476	3.337
7.60.....	13.868	11.406	9.310	7.757	6.334	5.078	3.880	2.828	1.790	0.918	0.111	1.079	2.522
7.70.....	15.000	12.838	10.610	8.899	7.316	5.895	4.531	3.309	2.108	1.078	0.139	0.774	1.862
7.80.....	15.000	14.252	11.891	10.026	8.289	6.714	5.191	3.808	2.454	1.274	0.208	0.555	1.339
7.90.....	15.000	15.000	13.187	11.172	9.282	7.552	5.875	4.337	2.839	1.517	0.326	0.420	0.939
8.00.....	15.000	15.000	14.496	12.341	10.308	8.431	6.605	4.915	3.272	1.809	0.491	0.360	0.648
8.10.....	15.000	15.000	15.000	13.505	11.334	9.319	7.352	5.520	3.740	2.141	0.698	0.363	0.445
8.20.....	15.000	15.000	15.000	14.659	12.356	10.207	8.105	6.137	4.227	2.497	0.931	0.411	0.308
8.30.....	15.000	15.000	15.000	15.000	13.369	11.089	8.858	6.758	4.722	2.865	1.177	0.488	0.217
8.40.....	15.000	15.000	15.000	15.000	14.367	11.962	9.603	7.376	5.217	3.236	1.428	0.580	0.155
8.50.....	15.000	15.000	15.000	15.000	15.000	12.820	10.338	7.986	5.707	3.603	1.677	0.681	0.113
8.60.....	15.000	15.000	15.000	15.000	15.000	13.665	11.061	8.587	6.189	3.965	1.922	0.786	0.084
8.70.....	15.000	15.000	15.000	15.000	15.000	14.509	11.786	9.192	6.677	4.333	2.173	0.897	0.062
8.80.....	15.000	15.000	15.000	15.000	15.000	15.000	12.489	9.778	7.148	4.686	2.411	1.006	0.047
8.90.....	15.000	15.000	15.000	15.000	15.000	15.000	13.177	10.349	7.605	5.027	2.639	1.112	0.036
9.00.....	15.000	15.000	15.000	15.000	15.000	15.000	13.853	10.911	8.053	5.361	2.859	1.215	0.028

NOTE.—Table 4 is available in its entirety in the electronic edition of the *Astrophysical Journal Supplement*. A portion is shown here for guidance regarding its form and content.

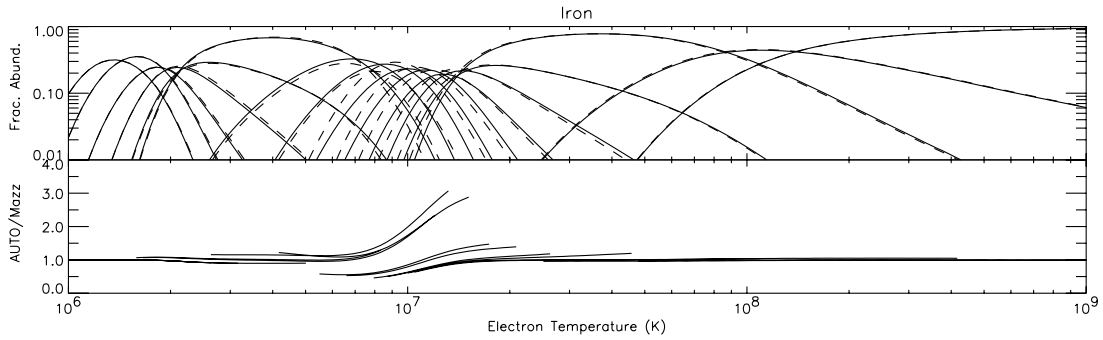

FIG. 2.26.—Ionization fractional abundance vs. electron temperature for Fe.

FIG. SET 2.—AUTOSTRUCTURE-based results. The solid curves of the upper graph show the ionization fractional abundance as calculated using the AUTOSTRUCTURE DR rate coefficients of Badnell (2006a) for H- through Na-like ions and the AUTOSTRUCTURE RR rate coefficients of Badnell (2006b) for bare through Na-like ions. We use the DR and RR rate coefficients of Mazzotta et al. (1998) for ions not calculated by Badnell (2006a, 2006b). The EII rate coefficients used are those of Mazzotta et al. (1998). The dashed curves show the abundances calculated by Mazzotta et al. (1998). The lower graph shows the ratio of the calculated abundances. The lowest ionization stage shown is P-like. Comparison is made only for fractional abundances greater than 10^{-2}. We label the results using the data of Badnell (2006a, 2006b) as "AUTO" and Mazzotta et al. (1998) as "Mazz." [*See the electronic version of the Supplement for Figs.* 2.1–2.30.]

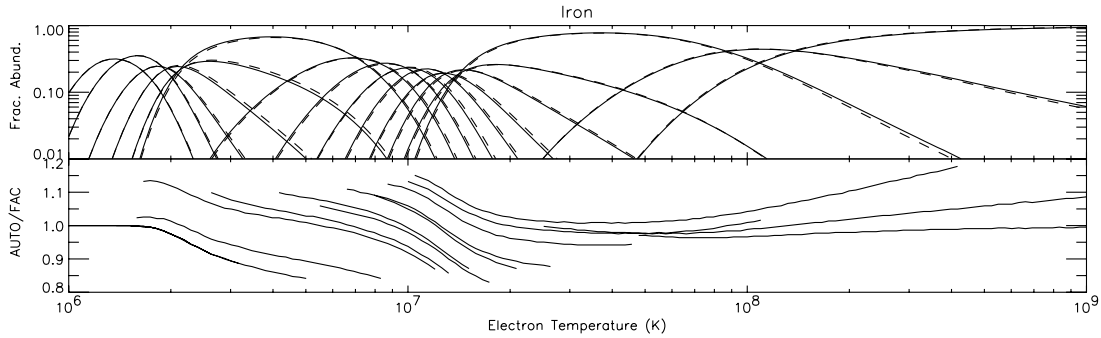

FIG. 3.6.—Ionization fractional abundance vs. electron temperature for Fe.

FIG. SET 3.—FAC-based results. The solid curves of the upper graph show the ionization fractional abundance as calculated using the AUTOSTRUCTURE DR rate coefficients of Badnell (2006a) for H- through Na-like ions and the AUTOSTRUCTURE RR rate coefficients of Badnell (2006b) for bare through Na-like ions. The dashed curves show the abundances as calculated using the FAC DR rate coefficients of Gu (2003b, 2004) for H- through Na-like ions and the FAC RR rate coefficients of Gu (2003a) for bare through F-like ions. We use the DR and RR rate coefficients of Mazzotta et al. (1998) for ions not calculated by Gu (2003a, 2003b, 2004) or by Badnell (2006a, 2006b). The EII rate coefficients used are those of Mazzotta et al. (1998). The lower graph shows the ratio of the calculated abundances. The lowest ionization stage shown is P-like. Comparison is made only for fractional abundances greater than 10^{-2}. We label the results using the data of Badnell (2006a, 2006b) as "AUTO" and Gu (2003a, 2003b, 2004) as "FAC." [*See the electronic version of the Supplement for Figs.* 3.1–3.7.]

We thus have a tridiagonal system in which the solution to all the ionization stage populations is given in terms of any one population. The system is tridiagonal since we consider only changes in charge state of $\Delta q = \pm 1$. Coupling equations (4) and (6) gives $Z + 2$ equations with $Z + 1$ unknowns. The set of equations are then degenerate, so we divide equation (6) by $N_{\rm tot} n_e$ and then arbitrarily replace the first row of equation (6) with equation (4). This set of equations is then solved using the ionization and recombination rate coefficients detailed previously. Our results are presented in terms of the calculated fractional abundances f.

8. RESULTS

Figure Set 2 (Figs. 2.1–2.28) show our calculated fractional abundances compared to those of Mazzotta et al. (1998). Mazzotta et al. did not publish results for the ionization balance of Cu and Zn, so we present our results without comparison (Figs. 2.29 and 2.30). Our calculated fractional abundances are given in tabular form in Table 4 with iron printed as an example. For the elements where DR and RR rate coefficients are also provided by Gu (2003b, 2003a, 2004), we compare the results using his data with those using the data of Badnell (2006a, 2006b). These comparisons are shown in Figure Set 3. The calculated fractional abundances based on the data of Gu are given in Table 5. To make these tables easily machine readable, we tabulate fractional abundances down to 10^{-15} and fix fractional abundances below this value to 10^{-15}.

We limit our studies to the temperature range 10^4–10^9 K. The recombination data of Badnell (2006a, 2006b) and Gu (2003b, 2003a, 2004) covers ionization stages from bare through Na-like. For ions with more electrons we use the data recommended by Mazzotta et al. (1998) and P. Mazzotta (2000, private communication). As the CIE calculations move to ionization stages with more electrons than Na-like, which has 11 electrons, the effects of the new DR and RR data decrease, as is expected. These differences become insignificant typically by the time one reaches the Si- or P-like isoelectronic sequence, with 14 and 15 electrons, respectively. Because of this, and to avoid figures becoming overly congested, we generally plot our results only for ionization stages with 15 or fewer electrons. The lower temperature limit shown is also increased to focus on these ionization stages. Where all ionization stages are not shown, the figure caption indicates such.

9. DISCUSSION

In the discussion below we point out differences in the CIE ionic fractional abundances we have calculated using the AUTOSTRUCTURE data of Badnell (2006a, 2006b) with calculations using other data. First, we compare to the recommended CIE results of Mazzotta et al. (1998), and then to the CIE results using the FAC data of Gu (2003b, 2003a, 2004). We highlight ions and temperatures where the differences are larger than 20%. The differences quoted are the percentage increase or decrease in our calculations relative to the fractional abundances of Mazzotta et al. (1998) or relative to those calculated using the data of Gu (2003b, 2003a, 2004). All differences discussed below can be attributed to the use of different DR and RR data sets.

To simplify the comparison, we point out where there are large differences at peak fractional abundance and at fractional abundances of 0.1 and 0.01. Table 6 lists ions where our peak abundances differ from those of Mazzotta et al. (1998) by more than 20%, or where the difference in peak formation temperature is $\geq$0.05 in the dex. This table gives the percentage change in peak fractional abundance and the change in temperature relative to the results of Mazzotta et al. (1998).

It is interesting to note that the differences in our calculated CIE fractional abundances relative to those of Mazzotta et al. (1998) are, in general, much larger than the differences between our results and the results using the data of Gu (2003b, 2003a, 2004). In the former case, peak abundance differences of nearly 60% are found (see Fig. 2.21) and the differences can be larger than a factor of 11 (i.e., 1000%) at fractional abundances down to 0.01 (see Fig. 2.17). For the latter case, peak abundance differences are within 10% and differences for fractional abundances down to 0.01 are within 50%. This reflects the fact that the modern DR and RR data are in better agreement with one another than with the older data.

We have not investigated the reliability of the DR and RR data at temperatures where the fractional abundance is $<$0.01; so our calculated fractional abundances must be used with caution outside this range. Comparison of the fractional abundances using the data of Badnell (2006a, 2006b) and Gu (2003b, 2003a, 2004) can be used to give an estimate of how the uncertainties in these modern DR and RR calculations translate into uncertainties in the CIE calculations for fractional abundances below 0.01.

TABLE 5

SAMPLE CIE FRACTIONAL ABUNDANCES (FAC-BASED RESULTS): IRON

log (T)	Fe^{0+}	Fe^{1+}	Fe^{2+}	Fe^{3+}	Fe^{4+}	Fe^{5+}	Fe^{6+}	Fe^{7+}	Fe^{8+}	Fe^{9+}	Fe^{10+}	Fe^{11+}	Fe^{12+}	Fe^{13+}
4.00	0.916	0.056	4.006	15.000	15.000	15.000	15.000	15.000	15.000	15.000	15.000	15.000	15.000	15.000
4.10	1.450	0.019	2.165	15.000	15.000	15.000	15.000	15.000	15.000	15.000	15.000	15.000	15.000	15.000
4.20	1.981	0.085	0.776	8.101	15.000	15.000	15.000	15.000	15.000	15.000	15.000	15.000	15.000	15.000
4.30	2.883	0.589	0.130	5.069	15.000	15.000	15.000	15.000	15.000	15.000	15.000	15.000	15.000	15.000
4.40	3.933	1.291	0.023	3.046	10.640	15.000	15.000	15.000	15.000	15.000	15.000	15.000	15.000	15.000
4.50	4.698	1.747	0.021	1.520	6.727	15.000	15.000	15.000	15.000	15.000	15.000	15.000	15.000	15.000
4.60	5.371	2.145	0.158	0.527	3.813	10.373	15.000	15.000	15.000	15.000	15.000	15.000	15.000	15.000
4.70	6.163	2.688	0.507	0.170	1.969	6.405	13.158	15.000	15.000	15.000	15.000	15.000	15.000	15.000
4.80	6.947	3.245	0.897	0.127	0.898	3.638	8.368	15.000	15.000	15.000	15.000	15.000	15.000	15.000
4.90	7.784	3.872	1.369	0.279	0.380	1.843	5.095	10.166	15.000	15.000	15.000	15.000	15.000	15.000
5.00	8.732	4.623	1.972	0.610	0.224	0.835	3.049	6.479	11.453	15.000	15.000	15.000	15.000	15.000
5.10	9.801	5.504	2.709	1.101	0.322	0.370	1.808	4.080	7.575	15.000	15.000	15.000	15.000	15.000
5.20	10.947	6.470	3.532	1.695	0.581	0.208	1.023	2.491	4.934	12.007	15.000	15.000	15.000	15.000
5.30	12.164	7.514	4.430	2.376	0.969	0.250	0.544	1.405	3.056	8.535	14.671	15.000	15.000	15.000
5.40	13.504	8.685	5.453	3.190	1.522	0.503	0.350	0.720	1.741	5.916	10.608	15.000	15.000	15.000
5.50	15.000	10.023	6.640	4.174	2.268	0.984	0.441	0.395	0.901	4.005	7.517	11.373	15.000	15.000
5.60	15.000	11.506	7.968	5.304	3.179	1.655	0.766	0.361	0.434	2.658	5.206	8.100	11.438	15.000
5.70	15.000	13.060	9.365	6.506	4.176	2.431	1.232	0.510	0.215	1.715	3.476	5.569	8.043	11.515
5.80	15.000	14.627	10.774	7.723	5.199	3.248	1.767	0.762	0.147	1.049	2.166	3.587	5.346	7.950
5.90	15.000	15.000	12.211	8.970	6.260	4.116	2.377	1.113	0.216	0.620	1.208	2.061	3.221	5.102
6.00	15.000	15.000	13.783	10.357	7.468	5.140	3.164	1.662	0.512	0.495	0.640	1.010	1.664	2.936
6.10	15.000	15.000	15.000	12.049	8.988	6.482	4.288	2.565	1.183	0.805	0.574	0.531	0.751	1.502
6.20	15.000	15.000	15.000	14.088	10.860	8.183	5.787	3.856	2.260	1.566	1.007	0.608	0.450	0.752
6.30	15.000	15.000	15.000	15.000	13.119	10.277	7.694	5.565	3.769	2.794	1.945	1.236	0.744	0.652
6.40	15.000	15.000	15.000	15.000	15.000	12.763	10.006	7.689	5.704	4.475	3.364	2.384	1.593	1.153
6.50	15.000	15.000	15.000	15.000	15.000	15.000	12.357	9.860	7.696	6.235	4.885	3.661	2.601	1.852
6.60	15.000	15.000	15.000	15.000	15.000	15.000	14.582	11.913	9.577	7.901	6.332	4.887	3.584	2.557
6.70	15.000	15.000	15.000	15.000	15.000	15.000	15.000	13.857	11.357	9.482	7.709	6.062	4.535	3.260
6.80	15.000	15.000	15.000	15.000	15.000	15.000	15.000	15.000	13.096	11.033	9.070	7.235	5.503	4.003
6.90	15.000	15.000	15.000	15.000	15.000	15.000	15.000	15.000	14.883	12.644	10.502	8.492	6.570	4.864
7.00	15.000	15.000	15.000	15.000	15.000	15.000	15.000	15.000	15.000	14.427	12.116	9.942	7.843	5.948
7.10	15.000	15.000	15.000	15.000	15.000	15.000	15.000	15.000	15.000	15.000	14.035	11.706	9.442	7.372
7.20	15.000	15.000	15.000	15.000	15.000	15.000	15.000	15.000	15.000	15.000	15.000	13.806	11.386	9.153
7.30	15.000	15.000	15.000	15.000	15.000	15.000	15.000	15.000	15.000	15.000	15.000	15.000	13.468	11.079
7.40	15.000	15.000	15.000	15.000	15.000	15.000	15.000	15.000	15.000	15.000	15.000	15.000	15.000	12.975
7.50	15.000	15.000	15.000	15.000	15.000	15.000	15.000	15.000	15.000	15.000	15.000	15.000	15.000	14.785
7.60	15.000	15.000	15.000	15.000	15.000	15.000	15.000	15.000	15.000	15.000	15.000	15.000	15.000	15.000
7.70	15.000	15.000	15.000	15.000	15.000	15.000	15.000	15.000	15.000	15.000	15.000	15.000	15.000	15.000
7.80	15.000	15.000	15.000	15.000	15.000	15.000	15.000	15.000	15.000	15.000	15.000	15.000	15.000	15.000
7.90	15.000	15.000	15.000	15.000	15.000	15.000	15.000	15.000	15.000	15.000	15.000	15.000	15.000	15.000
8.00	15.000	15.000	15.000	15.000	15.000	15.000	15.000	15.000	15.000	15.000	15.000	15.000	15.000	15.000
8.10	15.000	15.000	15.000	15.000	15.000	15.000	15.000	15.000	15.000	15.000	15.000	15.000	15.000	15.000
8.20	15.000	15.000	15.000	15.000	15.000	15.000	15.000	15.000	15.000	15.000	15.000	15.000	15.000	15.000
8.30	15.000	15.000	15.000	15.000	15.000	15.000	15.000	15.000	15.000	15.000	15.000	15.000	15.000	15.000
8.40	15.000	15.000	15.000	15.000	15.000	15.000	15.000	15.000	15.000	15.000	15.000	15.000	15.000	15.000
8.50	15.000	15.000	15.000	15.000	15.000	15.000	15.000	15.000	15.000	15.000	15.000	15.000	15.000	15.000
8.60	15.000	15.000	15.000	15.000	15.000	15.000	15.000	15.000	15.000	15.000	15.000	15.000	15.000	15.000
8.70	15.000	15.000	15.000	15.000	15.000	15.000	15.000	15.000	15.000	15.000	15.000	15.000	15.000	15.000
8.80	15.000	15.000	15.000	15.000	15.000	15.000	15.000	15.000	15.000	15.000	15.000	15.000	15.000	15.000
8.90	15.000	15.000	15.000	15.000	15.000	15.000	15.000	15.000	15.000	15.000	15.000	15.000	15.000	15.000
9.00	15.000	15.000	15.000	15.000	15.000	15.000	15.000	15.000	15.000	15.000	15.000	15.000	15.000	15.000

log (T)	Fe^{14+}	Fe^{15+}	Fe^{16+}	Fe^{17+}	Fe^{18+}	Fe^{19+}	Fe^{20+}	Fe^{21+}	Fe^{22+}	Fe^{23+}	Fe^{24+}	Fe^{25+}	Fe^{26+}
4.00	15.000	15.000	15.000	15.000	15.000	15.000	15.000	15.000	15.000	15.000	15.000	15.000	15.000
4.10	15.000	15.000	15.000	15.000	15.000	15.000	15.000	15.000	15.000	15.000	15.000	15.000	15.000
4.20	15.000	15.000	15.000	15.000	15.000	15.000	15.000	15.000	15.000	15.000	15.000	15.000	15.000
4.30	15.000	15.000	15.000	15.000	15.000	15.000	15.000	15.000	15.000	15.000	15.000	15.000	15.000
4.40	15.000	15.000	15.000	15.000	15.000	15.000	15.000	15.000	15.000	15.000	15.000	15.000	15.000
4.50	15.000	15.000	15.000	15.000	15.000	15.000	15.000	15.000	15.000	15.000	15.000	15.000	15.000
4.60	15.000	15.000	15.000	15.000	15.000	15.000	15.000	15.000	15.000	15.000	15.000	15.000	15.000
4.70	15.000	15.000	15.000	15.000	15.000	15.000	15.000	15.000	15.000	15.000	15.000	15.000	15.000
4.80	15.000	15.000	15.000	15.000	15.000	15.000	15.000	15.000	15.000	15.000	15.000	15.000	15.000
4.90	15.000	15.000	15.000	15.000	15.000	15.000	15.000	15.000	15.000	15.000	15.000	15.000	15.000
5.00	15.000	15.000	15.000	15.000	15.000	15.000	15.000	15.000	15.000	15.000	15.000	15.000	15.000
5.10	15.000	15.000	15.000	15.000	15.000	15.000	15.000	15.000	15.000	15.000	15.000	15.000	15.000

TABLE 5—*Continued*

log (T)	Fe^{14+}	Fe^{15+}	Fe^{16+}	Fe^{17+}	Fe^{18+}	Fe^{19+}	Fe^{20+}	Fe^{21+}	Fe^{22+}	Fe^{23+}	Fe^{24+}	Fe^{25+}	Fe^{26+}
5.20	15.000	15.000	15.000	15.000	15.000	15.000	15.000	15.000	15.000	15.000	15.000	15.000	15.000
5.30	15.000	15.000	15.000	15.000	15.000	15.000	15.000	15.000	15.000	15.000	15.000	15.000	15.000
5.40	15.000	15.000	15.000	15.000	15.000	15.000	15.000	15.000	15.000	15.000	15.000	15.000	15.000
5.50	15.000	15.000	15.000	15.000	15.000	15.000	15.000	15.000	15.000	15.000	15.000	15.000	15.000
5.60	15.000	15.000	15.000	15.000	15.000	15.000	15.000	15.000	15.000	15.000	15.000	15.000	15.000
5.70	15.000	15.000	15.000	15.000	15.000	15.000	15.000	15.000	15.000	15.000	15.000	15.000	15.000
5.80	10.923	14.448	15.000	15.000	15.000	15.000	15.000	15.000	15.000	15.000	15.000	15.000	15.000
5.90	7.281	9.903	11.983	15.000	15.000	15.000	15.000	15.000	15.000	15.000	15.000	15.000	15.000
6.00	4.439	6.294	7.648	13.279	15.000	15.000	15.000	15.000	15.000	15.000	15.000	15.000	15.000
6.10	2.421	3.621	4.431	8.719	13.687	15.000	15.000	15.000	15.000	15.000	15.000	15.000	15.000
6.20	1.162	1.807	2.216	5.456	9.254	13.654	15.000	15.000	15.000	15.000	15.000	15.000	15.000
6.30	0.617	0.797	0.905	3.329	6.206	9.572	13.407	15.000	15.000	15.000	15.000	15.000	15.000
6.40	0.728	0.524	0.391	2.171	4.324	6.872	9.803	13.151	15.000	15.000	15.000	15.000	15.000
6.50	1.084	0.565	0.226	1.487	3.062	4.960	7.171	9.730	12.556	15.000	15.000	15.000	15.000
6.60	1.488	0.704	0.179	1.012	2.114	3.488	5.119	7.042	9.171	11.553	14.004	15.000	15.000
6.70	1.923	0.913	0.214	0.681	1.388	2.329	3.486	4.891	6.450	8.229	10.035	15.000	15.000
6.80	2.428	1.217	0.353	0.503	0.871	1.445	2.205	3.179	4.268	5.551	6.822	14.605	15.000
6.90	3.075	1.682	0.657	0.527	0.598	0.856	1.276	1.884	2.578	3.445	4.271	10.485	15.000
7.00	3.964	2.402	1.222	0.840	0.645	0.624	0.747	1.040	1.395	1.909	2.363	7.305	12.945
7.10	5.210	3.489	2.157	1.545	1.111	0.839	0.698	0.712	0.774	0.983	1.126	5.036	9.598
7.20	6.827	4.953	3.473	2.649	1.996	1.496	1.117	0.883	0.685	0.629	0.514	3.584	7.266
7.30	8.598	6.579	4.954	3.934	3.077	2.368	1.772	1.313	0.883	0.593	0.267	2.650	5.608
7.40	10.348	8.186	6.418	5.213	4.168	3.263	2.468	1.803	1.165	0.667	0.164	1.982	4.342
7.50	12.020	9.721	7.814	6.435	5.212	4.125	3.144	2.290	1.461	0.776	0.120	1.470	3.331
7.60	13.623	11.190	9.148	7.604	6.212	4.954	3.799	2.768	1.764	0.908	0.114	1.070	2.512
7.70	15.000	12.616	10.440	8.739	7.187	5.766	4.446	3.250	2.083	1.067	0.143	0.764	1.849
7.80	15.000	14.024	11.717	9.862	8.156	6.582	5.106	3.753	2.433	1.266	0.215	0.545	1.323
7.90	15.000	15.000	13.011	11.007	9.150	7.421	5.792	4.289	2.824	1.513	0.337	0.411	0.923
8.00	15.000	15.000	14.324	12.179	10.178	8.304	6.528	4.877	3.266	1.813	0.509	0.355	0.633
8.10	15.000	15.000	15.000	13.349	11.211	9.198	7.283	5.493	3.745	2.154	0.723	0.362	0.432
8.20	15.000	15.000	15.000	14.511	12.241	10.095	8.046	6.122	4.243	2.520	0.965	0.415	0.298
8.30	15.000	15.000	15.000	15.000	13.263	10.987	8.809	6.756	4.751	2.899	1.220	0.496	0.208
8.40	15.000	15.000	15.000	15.000	14.273	11.871	9.567	7.387	5.258	3.280	1.480	0.593	0.148
8.50	15.000	15.000	15.000	15.000	15.000	12.742	10.314	8.011	5.761	3.659	1.738	0.698	0.107
8.60	15.000	15.000	15.000	15.000	15.000	13.600	11.050	8.626	6.257	4.033	1.991	0.807	0.079
8.70	15.000	15.000	15.000	15.000	15.000	14.458	11.788	9.246	6.758	4.414	2.252	0.922	0.058
8.80	15.000	15.000	15.000	15.000	15.000	15.000	12.506	9.846	7.242	4.779	2.498	1.035	0.044
8.90	15.000	15.000	15.000	15.000	15.000	15.000	13.208	10.431	7.713	5.132	2.735	1.144	0.033
9.00	15.000	15.000	15.000	15.000	15.000	15.000	13.898	11.006	8.175	5.478	2.964	1.251	0.026

NOTE.—Table 5 is available in its entirety in the electronic edition of the *Astrophysical Journal Supplement*. A portion is shown here for guidance regarding its form and content.

9.1. *First Row Elements*

The differences between our calculated fractional abundances and those of Mazzotta et al. (1998) for H are negligible. There is no DR process for H, and for the temperature range in Figure 2.1, the difference between the RR rate coefficients of Badnell (2006c) and Mazzotta et al. (1998) is less than 0.2% (which is better than the accuracy of the published RR rate coefficient fits). For He (Fig. 2.2), we find differences between our calculated fractional abundances and those of Mazzotta et al. to be within 20% for the neutral and singly ionized ion. Differences in the bare ion are negligible.

9.2. *Second Row Elements*

For Li and Be we find differences between our calculated fractional abundances relative to those of Mazzotta et al. (1998) to be within 20% for all ionization stages (Figs. 2.3 and 2.4, respectively). The difference for B is also of this order except for the neutral atom, where our calculations give an increase in abundance of ~50% at a fractional abundance of 0.1, rising to ~70% at 0.01 (Fig. 2.5). We attribute this to the B^{1+} DR rate coefficient calculated by Colgan et al. (2003) being almost an order of magnitude larger than that recommended by Mazzotta et al. in the CIE formation zone.

Differences for C (Fig. 2.6) are found to be generally within 20%. Exceptions are at temperatures of 1×10^4–2×10^4 K, where there are differences of up to 40% (but only for fractional abundances less than 0.1), and in the temperature range of 7×10^4–2×10^5 K, where the differences are up to 60% even at fractional abundances greater than 0.1.

For N (Fig. 2.7) we find the largest differences in the neutral and singly charged fractional abundances. These differences are found at temperatures of 1×10^4–3×10^4 K. They rise with decreasing fractional abundance to an ~140% increase in the neutral abundance and an ~80% decrease in singly charged abundance at fractional abundances of 0.1. Outside this temperature range, other ionization stages have differences within 50%. As in the B case, the increase in the neutral abundance and decrease in the singly charged abundance seen in our calculations is due to the N^{1+} DR rate coefficient of Zatsarinny et al. (2004a) being larger than that of Mazzotta et al. (1998).

For O (Fig. 2.8), the largest differences are found at temperatures of 6×10^4–4×10^5 K. For fractional abundances greater

TABLE 6

DIFFERENCE IN PEAK FRACTIONAL ABUNDANCE AND TEMPERATURE BETWEEN OUR AUTOSTRUCTURE-BASED CALCULATIONS AND THOSE OF MAZZOTTA ET AL. (1998)

Ion	Abundance Difference (%)	Temperature Difference (dex)	Temperature Difference (%)
F^{3+}	−17	0.05	12
Mg^{5+}	−24	−0.02	−4.5
Mg^{6+}	29	−0.03	−6.7
Al^{2+}	−32	0.02	4.7
Al^{6+}	−23	−0.03	−6.7
Al^{7+}	34	−0.04	−8.8
Al^{8+}	22	−0.01	−2.3
Si^{5+}	−27	0.04	9.6
P^{8+}	−26	0.00	0.0
S^{8+}	−5.2	0.05	12
S^{9+}	−42	0.02	4.7
Cl^{8+}	−7.2	0.05	12
Cl^{9+}	−8.6	0.06	15
Cl^{10+}	−47	0.03	7.2
K^{8+}	36	0.02	4.7
K^{11+}	22	0.06	15
K^{12+}	−41	0.05	12
Ca^{9+}	48	0.03	7.2
Ca^{11+}	21	0.03	7.2
Ca^{12+}	29	0.07	17
Ca^{13+}	−40	0.06	15
Ca^{14+}	−24	0.04	9.6
Sc^{10+}	57	0.03	7.2
Sc^{14+}	−22	0.02	4.7
Ti^{15+}	−21	0.03	7.2
V^{12+}	25	0.01	2.3
Mn^{16+}	22	0.02	4.7
Mn^{20+}	−21	0.02	4.7
Fe^{18+}	28	0.03	7.2
Fe^{19+}	−26	0.03	9.6
Co^{18+}	28	0.03	7.2
Co^{19+}	48	0.05	12
Co^{20+}	−37	0.05	12
Co^{21+}	−21	0.04	9.6
Co^{22+}	−26	0.02	4.7
Ni^{19+}	34	0.04	9.6
Ni^{20+}	61	0.06	15
Ni^{21+}	−42	0.07	17
Ni^{22+}	−25	0.05	12
Ni^{23+}	−24	0.04	9.6

NOTES.—We list here ions showing a difference that is >20% between peak fractional abundance from our calculations and those of Mazzotta et al. (1998) or have a difference in peak formation temperature that is $\geq$0.05 in the dex. For each ion we list the percentage change compared to the Mazzotta et al. (1998) results, with positive values indicating an increase and negative indicating a decrease. Also listed is the change in the dex and the percentage change of the temperature at which the fractional abundance peaks.

than 0.1, the difference is as large as a 40% decrease for the singly charged ion. The difference is within 30% for the other ions. When fractional abundances as low as 0.01 are considered, the decrease in the singly charged abundance is up to 60%.

Of all the second row elements, F (Fig. 2.9) shows the largest deviation from the Mazzotta et al. (1998) results. This difference is most pronounced for the first four ionization stages. In particular, at temperatures of 1×10^4–3×10^4 K we find differences up to 120% for fractional abundances from 0.1 to 0.01. Also for these four ions, at temperatures of 7×10^4–3×10^5 K the differences are ~200% for fractional abundances down to 0.1, and nearly 300% for abundances down to 0.01.

Ne (Fig. 2.10) shows differences of up to 100% at fractional abundances of 0.1. The largest of these is in the temperature range 1×10^5–4×10^5 K, where the Ne^{3+} abundance is decreased relative to the Mazzotta et al. (1998) results and the Ne^{4+} abundance is increased.

9.3. *Third Row Elements*

We find relatively small differences for Na (less than 30%), except for Na^{3+}, Na^{4+}, and Na^{5+} at temperatures of 2×10^5–7×10^5 K (Fig. 2.11). In this temperature range for Na^{3+} we find a decrease of ~120% in the fractional abundance at 0.1 and ~200% in the fractional abundance at 0.01. For Na^{4+} and Na^{5+}, increases of ~60% are seen at a fractional abundance of 0.1.

The largest differences in Mg peak abundance (Fig. 2.12) are for Mg^{5+}, which shows a 24% decrease relative to Mazzotta et al. (1998), and Mg^{6+}, which shows a 29% increase. Off peak, the largest difference for Mg is in the neutral atom. At 1×10^4–2×10^4 K, for fractional abundances between 0.01 and 0.4, our results are larger then those of Mazzotta et al. (1998) by between 160% and 250%. This is due to the Mg^{1+} DR and RR rate coefficients of Altun et al. (2006) and Badnell (2006b), respectively, being around a factor of 2 larger than those recommended by Mazzotta et al. (1998). Other differences for Mg are concentrated around the 3×10^5–2×10^6 K temperature range, where they are up to 100%.

Differences in our fractional abundance curves relative to those of Mazzotta et al. (1998) for Al (Fig. 2.13) are seen across a wide range of ionization stages. Al^{2+} shows a 32% decrease in peak abundance, Al^{6+} shows a 23% decrease, Al^{7+} shows a 34% increase, and Al^{8+} shows a 22% increase. At a fractional abundance of 0.1, the maximum difference is ~150% for all ions.

For Si (Fig. 2.14), the peak abundance of Si^{5+} is decreased by 27%. The differences seen for Si are up to 70% relative to Mazzotta et al. (1998) for all but the F- and Ne-like ions. These two ions show differences of over 200% at fractional abundances of 0.1 and temperatures between 2×10^5 and 6×10^5 K.

The largest difference in peak abundance for P (Fig. 2.15) is P^{8+}, which shows a 26% decrease relative to the results of Mazzotta et al. (1998). Other differences in abundance between our results and Mazzotta et al. (1998) for P are largest at 3×10^5–3×10^6 K. In particular, P^{5+} shows an increase of ~140% at a fractional abundance of 0.1, and of ~250% at an abundance of 0.01.

S, Cl, and Ar (Figs. 2.16, 2.17, and 2.18, respectively) show the greatest peak abundance difference in the N-like ion. The decrease for S^{9+} is 42% relative to the fractional abundance of Mazzotta et al. (1998), for Cl^{10+} it is 47%, and for Ar^{11+} it is 14%. Also, the temperature of peak formation of Cl^{9+} is increased by 0.06 in the dex. These three elements all show maximum discrepancy in the temperature range 6×10^5–3×10^6 K. For S these differences are up to a factor of 3 at fractional abundances of 0.1, and up to a factor of 6 at fractional abundances of 0.01. For Cl these differences are up to a factor of 4.2 at fractional abundances of 0.1, and up to a factor of 11 at fractional abundances of 0.01. For Ar these differences are no greater than a factor of 1.5 for fractional abundances of 0.1 and up to a factor of 2 at fractional abundances of 0.01.

Figure 3.1 shows the differences in fractional abundances calculated using the data of Badnell (2006a, 2006b) compared to the data of Gu (2003b, 2003a, 2004) for Mg. These differences are up to 30% for fractional abundances of 0.1 and greater, and up to 50% for fractional abundances of 0.01. They are concentrated in temperature regions of 1×10^4–2×10^4 and 3×10^5–2×10^6 K. Comparison with the calculated abundances of Si (Fig. 3.2) shows differences up to 25% at fractional abundances of 0.1,

rising to ~30% at abundances of 0.01. S and Ar abundances were also calculated using the data of Gu. Agreement here for S (Fig. 3.3) is within 25% at an abundance of 0.1 and 40% at an abundance of 0.01. For Ar (Fig. 3.4), the agreement is within 20% at an abundance of 0.1 and 30% at an abundance of 0.01. For S and Ar, the largest difference is seen for the Ne- and Mg-like ions.

9.4. *Fourth Row Elements*

For K and Ca (Figs. 2.19 and 2.20, respectively), the largest peak abundance differences are for the Na-, O-, and N-like ions. For Na-like K^{8+} the increase is 36% relative to Mazzotta et al. (1998), and for Ca^{9+} it is 48%. For O-like K^{11+} the increase is 22%, and for Ca^{12+} it is 29%. For N-like K^{12+} the decrease is 41% relative to Mazzotta et al. (1998), and for Ca^{13+} it is 40%. Large increases in the temperature of peak abundance are found for K^{11+}, Ca^{12+} and Ca^{13+}; they are 0.06, 0.07, and 0.06 in the dex, respectively. For these elements the largest fractional abundance differences are seen between 2×10^6 and 6×10^6 K and are within a factor of 5 at fractional abundances of 0.1 and up to a factor of 8 at fractional abundances of 0.01.

Differences between our results and those of Mazzotta et al. (1998) for Sc (Fig. 2.21) at peak abundance are a 57% increase for Sc^{10+} and a 21% decrease for Sc^{14+}. Differences for all ions are up to 80% at fractional abundances of 0.1, and 150% for fractional abundances of 0.01. The largest differences are between 7×10^5 and 1×10^7 K.

The largest Ti and V peak abundance differences (Figs. 2.22 and 2.23, respectively) are a 21% decrease for Ti^{15+} and a 25% increase for V^{12+}. These elements show differences in fractional abundance from our calculations relative to those of Mazzotta et al. (1998) concentrated at temperatures of $3 \times 10^6 - 1 \times 10^7$ K. These differences are less than a factor of 2 for fractional abundances of 0.1 and above. They are up to a factor of 3 at fractional abundances of 0.01.

Cr, Mn, and Fe (Figs. 2.24, 2.25, and 2.26, respectively) all show similar differences relative to the Mazzotta et al. (1998) data. Of these elements, the largest percentage difference in peak abundance is seen for the Fe^{18+} ion, which has an increase of 28%. Other differences for these three elements are in the temperature range $4 \times 10^6 - 2 \times 10^7$ K and are up to a factor of 2.2 at fractional abundances of 0.1 and a factor of 3 at fractional abundances of 0.01.

Co and Ni (Figs. 2.27 and 2.28, respectively) have a number of ions with large differences in peak fractional abundances relative to Mazzotta et al. (1998). For Co, the largest of these are Co^{19+}, which has a 48% increase in peak abundance, and Co^{20+}, which has a 37% decrease. The temperature of peak formation is also increased by 0.05 in the dex in both cases. The largest peak abundance differences for Ni are for Ni^{19+}, Ni^{20+}, and Ni^{21+}, with a 34% increase, a 61% increase, and a 42% decrease, respectively. Ni^{20+} and Ni^{21+} also have an increase in peak abundance temperature of 0.06 and 0.07 in the dex, respectively. Both Co and Ni show the largest discrepancies between our results and those of Mazzotta et al. (1998) between 7×10^6 and 2×10^7 K. For Co these differences are up to a factor of 3.5 at fractional abundances of 0.1 and up to a factor of 4 at fractional abundances of 0.01. For Ni they are up to a factor of 4 at fractional abundances of 0.1 and up to a factor of 7 at fractional abundances of 0.01.

In Figures 2.29 and 2.30 we present the ionization fractional abundances of Cu and Zn without comparison. We note that Mazzitelli & Mattioli (2002) present fractional abundance results for these elements using updated ionization rate coefficients, but the purpose of our present work is to highlight the effect of improved recombination data. Comparison to Mazzitelli & Mattioli (2002) will be considered in a future work where we include updated EII data.

Comparing with Ca abundances from the data of Gu (2003b, 2003a, 2004) gives differences not larger than 20% at fractional abundances of 0.1 and not larger than 30% at fractional abundances of 0.01 for all temperatures covered here (Fig. 3.5). Comparing for Fe gives differences in the fractional abundance that are within 20% at all temperatures (Fig. 3.6). For Ni, differences in the fractional abundance are within 15% at fractional abundances of 0.1 and 25% at fractional abundances of 0.01 (Fig. 3.7).

10. CONCLUSION

This work has collected the most recent state-of-the-art theoretical DR and RR rate coefficients and, based on these data, calculated new CIE ionic fractional abundances of all elements from H to Zn. For these elements we have implemented the data of Badnell (2006a, 2006b) for all charge states from bare through Na-like. DR data for Mg, Si, S, Ar, Ca, Fe, and Ni have also been calculated by Gu (2003b, 2004) for all charge states from H- through Na-like. In addition, RR data for these seven elements has been calculated by Gu (2003a) for all charge states from bare through F-like. We have also computed ionization balance results using these data of Gu. For ionization stages not provided by the above calculations, we revert to the recombination data recommended by Mazzotta et al. (1998) for all elements up to and including Ni, and those recommended by P. Mazzotta (2000, private communication) for Cu and Zn. We also use the EII data from these two sources.

Our results represent a significant improvement over past CIE calculations. This will impact directly on the plasma conditions inferred from spectral observations and is thus of much importance for the astrophysics community. We will further this study in subsequent work by the inclusion of experimentally derived DR data for singly and doubly charged ions (where available), incorporating CT, and updating the EII data to the extent possible.

We conclude by noting that further progress in CIE calculations will require a concerted theoretical and experimental effort to generate the remaining needed atomic data. Modern DR and RR data are urgently needed for ions with 12 or more bound electrons. There is also a need for improved EII and CT data. There has been no significant revision or laboratory benchmarking of the recommended EII database since around 1990. In addition, the latest compilation of recommended CT rate coefficients dates back to Kingdon & Ferland (1996). This is in need of updating to reflect advances in CT in the last decade. We propose that all future data for DR, RR, CT, and EII should be generated aiming for an accuracy of better than 35%. This will match the accuracy of the modern electron-ion recombination measurements and calculations and help to ensure a uniformity of accuracy for future CIE calculations. Such an accurate and up-to-date database is crucial for being able to produce reliable CIE calculations for the astrophysics community.

We thank M. Bannister, M. Finkenthal, T. Kato, E. Landi, S. Loch, M. Mattioli, P. Mazzotta, and R. Smith for stimulating conversations. P. B., T. W. G., W. M., and D. W. S. were supported in part by the NASA Solar and Heliospheric Physics Supporting Research and Technology program and the NASA Astronomy and Physics Research and Analysis Program. N. R. B. was supported in part by PPARC PPA\G\S2003\00055. J. M. L. was supported by NASA LWS Contract NNH05AAOSI and by Basic Research Funds of the Office of Naval Research.

REFERENCES

Altun, Z., Yumak, A., Badnell, N. R., Colgan, J., & Pindzola, M. S. 2004, A&A, 420, 775 (erratum 433, 395 [2005])
Altun, Z., Yumak, A., Badnell, N. R., Loch, S. D., & Pindzola, M. S. 2006, A&A, 447, 1165
Arnaud, M., & Raymond, J. C. 1992, ApJ, 398, 394
Arnaud, M., & Rothenflug, R. 1985, A&AS, 60, 425
Badnell, N. R. 1986, J. Phys. B, 19, 3827
———. 2006a, Atomic and Molecular Diagnostic Processes in Plasmas (Dept. Physics, Univ. Strathclyde), http://amdpp.phys.strath.ac.uk/tamoc/DR/
———. 2006b, Atomic and Molecular Diagnostic Processes in Plasmas (Dept. Physics, Univ. Strathclyde), http://amdpp.phys.strath.ac.uk/tamoc/RR/
———. 2006c, A&A, 447, 389
———. 2006d, ApJS, submitted (astro-ph/0604144)
Badnell, N. R., et al. 2003, A&A, 406, 1151
Bautista, M. A., & Badnell, N. R. 2006, A&A, submitted
Beiersdorfer, P. 2003, ARA&A, 41, 343
Bell, K. L., Gilbody, H. B., Hughes, J. G., Kingston, A. E., & Smith, F. J. 1983, J. Phys. Chem. Ref. Data, 12, 891
Colgan, J., Pindzola, M. S., & Badnell, N. R. 2004, A&A, 417, 1183 (erratum 429, 369 [2005])
Colgan, J., Pindzola, M. S., Whiteford, A. D., & Badnell, N. R. 2003, A&A, 412, 597
DeWitt, D. R., Schuch, R., Gao, H., Asp., S., Biedermann, C., Chen, M. H., & Badnell, N. R. 1996, Phys. Rev. A, 53, 2327
Fogle, M., Badnell, N. R., Eklöw, N., Mohamed, T., & Schuch, R. 2003, A&A, 409, 781
Fogle, M., Badnell, N. R., Glans, P., Loch, S. D., Madzunkov, S., Abdel-Naby, Sh., A., Pinidzola, M. S., & Schuch, R. 2005, A&A, 442, 757
Gorczyca, T. W., & Badnell, N. R. 1997, Phys. Rev. Lett., 79, 2783
Gorczyca, T. W., Kodituwakka, C. N., Korista, K. T. Zatsarinny, O., Badnell, N. R., Behar, E., Chen, M. H., & Savin, D. W. 2003, ApJ, 592, 636
Gu, M. F. 2003a, ApJ, 589, 1085
———. 2003b, ApJ, 590, 1131
———. 2004, ApJS, 153, 389
Higgins, M. J., et al. 1989, Culham Lab. Rep. CLM-R 294
Kaastra, J. S., & Mewe, R. 1993, A&AS, 97, 443
Kato, T., Masai, K., & Arnaud, M. 1991, National Institute for Fusion Science NIFS-DATA-14
Kingdon, J. B., & Ferland, G. J. 1996, ApJS, 106, 205
Landi, M., & Monsignori Fossi, B. C. 1991, A&AS, 91, 183
Lennon, M. A., Bell, K. L., Gilbody, H. B., Hughes, J. G., Kingston, A. E. Murray, M. J., & Smith, F. J. 1988, J. Phys. Chem. Ref. Data, 17, 1285
Linkemann, J., Müller, A., Kenntner, J., Habs, D., Schwalm, D., Wolf, A., Badnell, N. R., & Pindzola, M. S. 1995, Phys. Rev. Lett., 74, 4173
Loch, S. D., Ludlow, J. A., Pindzola, M. S., Whiteford, A. D., & Griffin, D., C. 2005, Phys. Rev. A, 72, 2716
Lotz, W. 1968, Z. Phys., 216, 241
Masai, K. 1997, A&A, 324, 410
Mazzitelli, G., & Mattioli, M. 2002, At. Data Nucl. Data Tables, 82, 313
Mazzotta, P., Mazzitelli, G., Colafrancesco, S., & Vittorio, N. 1998, A&AS, 133, 403
Mitnik, D. M., & Badnell, N. R. 2004, A&A, 425, 1153
Müller, A. 1995, in Atomic and Plasma-Material Interaction Data for Fusion, Suppl. to Nucl. Fusion, Vol. 6 (Vienna: IAEA), 59
———. 1999, Int. J. Mass Spectr., 192, 9
Müller, A., & Wolf, A. 1997, in Accelerator-based Atomic Physics Techniques and Applications, ed. S. M. Shafroth & J. C. Austin (New York: AIP), 147
Nahar, S., N. 1999, ApJS, 120, 131
———. 2005a, ApJS, 156, 93
———. 2005b, ApJS, 158, 80
———. 2006, ApJS, 164, 280
Nahar, S., N., & Pradhan, A., K. 1997, ApJS, 111, 339
———. 2003, ApJS, 149, 239
———. 2006, ApJS, 162, 417
Nahar, S., N., Pradhan, A. K., & Zhang, H. L. 2000, ApJS, 131, 375
———. 2001, ApJS, 133, 255
Nussbaumer, H., & Storey, P. J. 1983, A&A, 126, 75
Pindzola, M. S., Badnell, N. R., & Griffin, D. C. 1992, Phys. Rev. A, 46, 5725
Pindzola, M. S., & Buie, M. J. 1988, Phys. Rev. A, 37, 3232
Pindzola, M. S., Griffin, D. C., Bottcher, C., Younger, S. M., & Hunter, H. T. 1987, Nucl. Fusion, Special Supp., 21
Pradhan, A. K., Chen, G., X., Nahar, S. N., & Zhang, H., L. 2001, Phys. Rev. Lett., 87, 183201
Savin, D. W., & Laming, J. M. 2002, ApJ, 566, 1166
Savin, D. W., et al. 1997, ApJ, 489, L115
———. 1999, ApJS, 123, 687
———. 2003, ApJS, 147, 421
———. 2006, ApJ, 642, 1275
Schippers, S. 1999, Phys. Scr., 80, 158
Seaton, M. J., & Storey, P. J. 1976, Atomic Processes and Applications, ed. P. G. Burke & B. L. Moiseiwitsch (Amsterdam: North Holland), 133
Shull, J. M., & van Steenberg, M. 1982, ApJS, 48, 95 (erratum 49, 351)
Verner, D. A., & Ferland, G. J. 1996, ApJS, 103, 467
Zatsarinny, O., Gorczyca, T. W., Fu, J., Korista, K. T., Badnell, N. R., & Savin, D. W. 2006, A&A, 447, 379
Zatsarinny, O., Gorczyca, T. W., Korista, K. T., Badnell, N. R., & Savin, D. W. 2003, A&A, 412, 587 (erratum 438, 743 [2005])
———. 2004a, A&A, 417, 1173 (erratum 440, 1203 [2005])
———. 2004b, A&A, 426, 699